Universidade do Minho
Escola de Ciências

João Miguel Fernandes Araújo

Behaviour of lactoferrin nanohydrogels incorporating curcumin as model compound into food simulants

outubro de 2018

Behaviour of lactoferrin nanohydrogels incorporating curcumin as model compound into food simulants
João Miguel Fernandes Araújo
Uminho | 2018

Universidade do Minho
Escola de Ciências

João Miguel Fernandes Araújo

Behaviour of lactoferrin nanohydrogels incorporating curcumin as model compound into food simulants

Master thesis
Master's degree in Biophysics and Bionanosystems

Supervisors
Óscar Leandro da Silva Ramos, PhD
Paulo José Gomes Coutinho, PhD

October 2018

Acknowledgements

O desenvolvimento desta tese de mestrado deve-se não só ao meu esforço, trabalho e dedicação, como também a todas as pessoas que me ajudaram e colaboraram de alguma forma, bem como a instituição e as escolas que tornaram isto possível.

Em primeiro quero deixar um agradecimento muito especial aos meus orientadores. Ao Óscar Ramos, ao Professor António Vicente, à Ana Isabel e ao Professor Paulo Coutinho, um grande obrigado e um abraço especial por terem acreditado em mim, por tudo o que me ensinaram e pela amizade.

À Escola de Ciências, ao Centro de Engenharia Biológica (CEB) da Universidade do Minho e à anterior e atual direção de mestrado, deixo um especial agradecimento pelo suporte, pelos recursos e pelos espaços que foram necessários para a realização deste trabalho. Como tal, agradeço a todos os técnicos que de alguma forma colaboraram neste trabalho, especialmente à técnica Paula Pereira.

Ao Laboratório de Indústria e Processos (LIP) e a todos os que fazem parte desta família, deixo um grande abraço e um obrigado por tudo, tudo mesmo...em especial ao Rui, à Lívia e ao Daniel por todo o conhecimento e sabedoria que me passaram, à Sara, Luís, Pedro, Maciel, Maria (Kiki), Rafaela, Ricardo, Joana, Arlete, Raquel, Zita, Michel, Luiz e Yeimy. Foi um prazer conhecer-vos e trabalhar ao vosso lado!

Quero deixar um grande abraço ao Lautas, ao Mário e ao Xarepe por toda a amizade e apoio que me deram ao longo desta jornada.

Deixo um grande abraço e um agradecimento ao Rómulo, à Sara e aos investigadores do Laboratório de Biotecnologia Molecular (LBM) pela cedência de equipamentos, bem como ao Professor Luís Vieira do Departamento de Física da Escola de Ciências, ao Professor Luís Abrunhosa do CEB e ao Rui Fernandes do IBMC pela colaboração em análises importantes para a execução deste trabalho.

Por último, mas não menos importante, quero agradecer e deixar um grande beijo e abraço à minha família (Pai, mãe e irmã) e à minha namorada Joana por todo o amor e paciência, e aos meus amigos por me ouvirem e por toda a amizade.

Behaviour of lactoferrin nanohydrogels incorporating curcumin as model compound into food simulants

Abstract

Food-grade nanostructures can be used as vehicles for the incorporation of nutraceutical agents (e.g., antioxidants or vitamins) aiming at the development of functional foods. These nanostructures provide higher protection, stability and controlled release to such nutraceutical agents. Fundamental knowledge regarding nanostructures behaviour when associated with nutraceuticals and their interactions with real food matrices is essential. In this study, a lactoferrin (LF) nanohydrogel was developed to encapsulate curcumin (nutraceutical model) aiming at its behaviour evaluation. The release kinetics of curcumin from LF nanohydrogels were also assessed by using food simulants (i.e., hydrophilic medium (ethanol 10 %) and lipophilic medium (ethanol 50 %), according to the commission Regulation (EU) No 10/2011). LF nanohydrogel isolated and loaded with curcumin was comprehensively characterized resorting to several techniques such as dynamic light scattering (DLS), fluorometry, circular dichroism (CD), Fourier-transform infrared spectroscopy (FTIR), transmission electron microscopy (TEM) and native electrophoresis. These LF-curcumin nanohydrogels were studied at a spectroscopic level when incorporated into gelatine (food model matrix). This system was able to associate curcumin at 80 μg/mL with a remarkable efficiency of ca. 90 % and loading capacity of ca. 3 %. Within fluorometric characterization, it was suggested that LF and curcumin molecules bind through hydrophobic interactions and FRET (Fluorescence resonance energy transfer) occurrence allowed the determination of *r* distance between curcumin chromophores and the nearest LF hydrophobic residues at the binding site. Under refrigerated conditions (4 °C), this system is stable up to 35 days, while at room temperature (25 °C) it has shown to be stable up to 14 days of storage. LF nanohydrogel presented higher release rates of curcumin in a lipophilic food simulant (after ca. 7 h) in comparison with a hydrophilic one (after ca. 4 h). LF nanohydrogels were successfully incorporated in a gelatine matrix and the respective characterization indicated that LF and curcumin molecules did not show any degradation in this process. The physicochemical characterization of LF-curcumin nanohydrogels gave rise to valuable information in what binding, interactions and stability concerns. Finally, the behaviour of this system as well as curcumin release kinetics in food simulants endows LF nanohydrogel as an interesting system to associate with lipophilic nutraceuticals and to incorporate in refrigerated food products with hydrophilic character.

Comportamento de nanohidrogéis de lactoferrina incorporando curcumina como composto modelo em simuladores alimentares

Resumo

Nanoestruturas de grau alimentar podem ser utilizadas como veículos para a incorporação de agentes nutracêuticos (como antioxidantes ou vitaminas) visando o desenvolvimento de alimentos funcionais. Estas nanoestruturas conferem maior proteção, estabilidade e libertação controlada a tais agentes. É necessário um conhecimento fundamental face a estas nanoestruturas, visando compreender o seu comportamento quando associadas a nutracêuticos e a sua interação com matrizes alimentares. Neste trabalho, um nanohidrogel de lactoferrina (LF) foi desenvolvido para encapsular curcumina (modelo de composto nutracêutico), visando a avaliação do seu comportamento. As cinéticas de libertação da curcumina a partir dos nanohidrogéis de LF foram realizadas quando adicionados a simuladores alimentares (meio hidrofílico (etanol 10 %) e meio lipofílico (etanol 50 %)) (De acordo com a COMISSÃO REGULAMENTAR da UE n.º 10/2011). O nanohidrogel de proteína isolado e carregado com curcumina foi caracterizado recorrendo a diversas técnicas tais como DLS, fluorimetria, DC, FTIR, TEM e eletroforese. Os nanohidrogéis de LF-curcumina foram introduzidos numa gelatina modelo, e estudados a um nível espectroscópico. Este sistema foi capaz de associar curcumina a 80 μg/mL com uma notável eficiência de ~ 90% e capacidade de carga de ~ 3%. Na caracterização fluorométrica, sugeriu-se que as moléculas de LF e curcumina se ligam através de interações hidrofóbicas e, a ocorrência de FRET permitiu a determinação da distância entre os cromóforos de curcumina e os resíduos hidrofóbicos de LF mais próximos no local de ligação. Sob condições refrigeradas (4 ° C), este sistema é estável até 35 dias, enquanto que à temperatura ambiente (25 ° C) mostrou ser estável apenas até aos 14 dias de armazenamento. O nanohidrogel de LF apresentou taxas de libertação de curcumina superiores num simulador alimentar lipofílico (após ~ 7 horas) em comparação com um hidrofílico (após ~ 4 horas). Estas nanoestruturas foram incorporadas com sucesso numa gelatina e a respetiva caracterização indicou que quer a LF quer a curcumina não apresentaram degradação. A caracterização físico-química das mesmas permitiu a obtenção de informação valiosa no que às interações e estabilidade concerne. Finalmente, o comportamento deste sistema, bem como a cinética de libertação da curcumina em simuladores alimentares, dotam os nanohidrogéis de LF num sistema interessante para se associar a nutracêuticos lipofílicos e para incorporar em produtos alimentares refrigerados com carácter hidrofílico.

TABLE OF CONTENTS

List of figures

List of tables

General classification list

Abbreviations

Symbols

CHAPTER 1 – MOTIVATION AND OBJECTIVE

1.1. Motivation

The aging process and the growing appearance of chronic and cardiovascular diseases are public concerns that scientists are trying to address either by using new technologies or by developing novel strategies to delay or even overcome these issues. The use of nutraceuticals with proved health benefits may represent one of the possible solutions to prevent the development or the evolution of these pathologies. Nonetheless, a great number of antioxidant agents, due to their intrinsic reactive nature, cannot be used directly in their pure state. In this sense, the general motivation of this study is to serve this purpose by exploring the technological potential of whey protein nanostructures for the encapsulation of nutraceuticals, intended the development of innovative functional foods. However, due to the lack of information regarding the incorporation of nanostructures in foods, an elucidation of how these protein nanostructures behave when in contact with food matrices is needed, before their application in functional foods field. Meaning this, the main motivation of this thesis is to evaluate the behaviour of a specific LF nanohydrogel loaded with a model nutraceutical, in food simulants as well as to understand the phenomena involved. Therefore, for a proper comprehension and to obtain accurate results, this study contemplates several essential steps (detailed in the next section) towards specific objectives, which are expected to be achieved. With the results of this thesis it is also expected to improve knowledge on the application of nanostructures to foods (food simulants and real food matrices), thus promoting the utilization of edible and food-grade materials from renewable sources – which are important emerging areas in the food industry.

The schematic representation of the work developed during this thesis

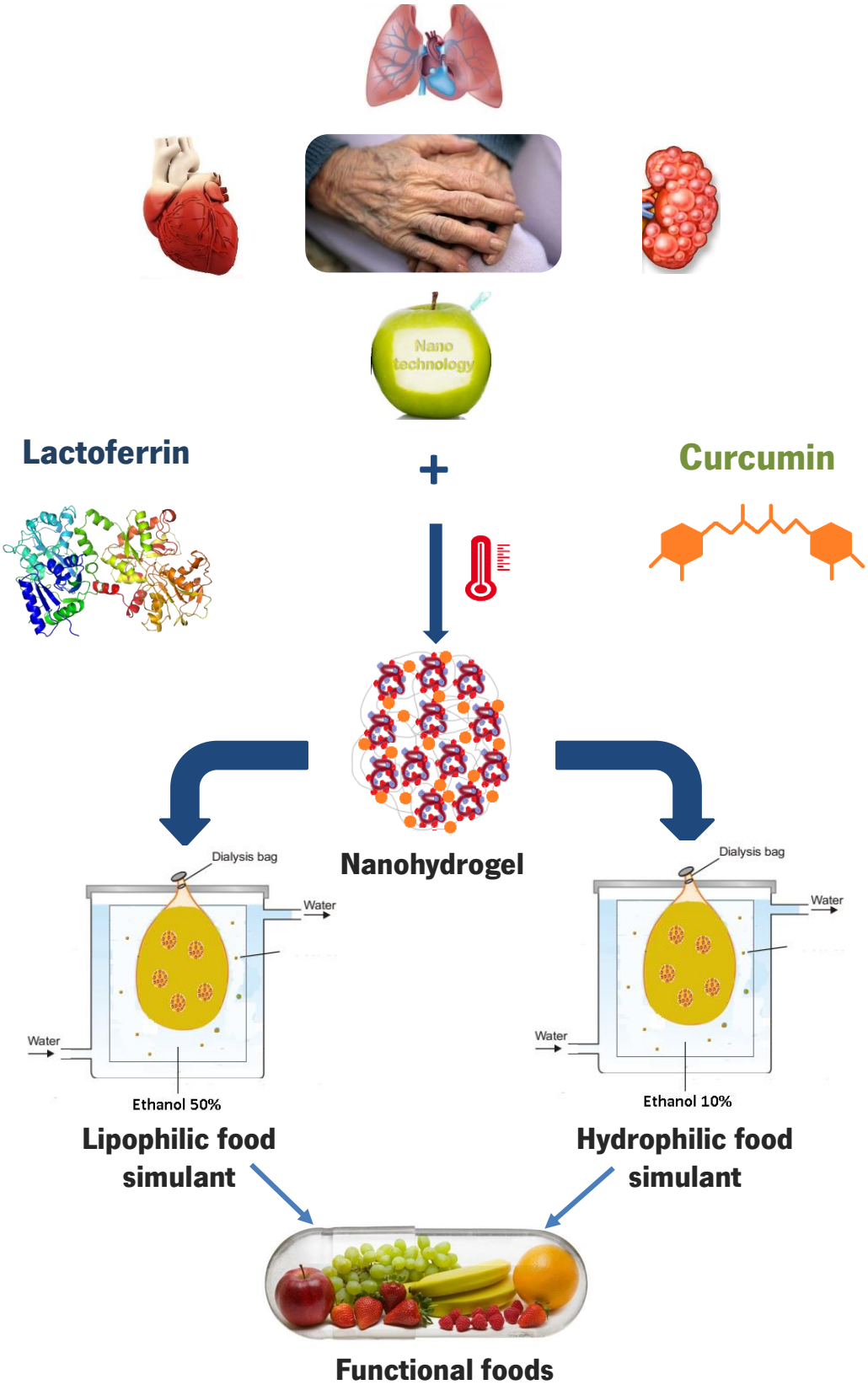

1.2. Objective

The main aim of this work is to evaluate the behaviour of a LF nanohydrogel and of a model nutraceutical incorporated into it, in food simulants and real food matrices. This goal was achieved through the following steps:

- Evaluation of the association efficiency of a nutraceutical model (i.e., curcumin) in nanostructures (i.e., nanohydrogels) developed from a whey protein, lactoferrin (LF);

- Evaluation of the physicochemical properties of LF nanohydrogels loaded with curcumin, under environmental conditions;

- Evaluation and comprehension of LF nanohydrogels-curcumin interactions at a spectroscopic level;

- Evaluation of curcumin' release kinetics in food simulants;

- Evaluation of the behaviour of LF nanohydrogels loaded with curcumin when added into real food matrices (i.e., gelatine and olive oil).

CHAPTER 2 - STATE OF THE ART

2.1. Introduction

Nanotechnology refers to the manipulation of matter on an atomic and/or molecular level. It involves the design, production, processing and application of materials through their control of size and shape at the nanometre scale. The main benefits of nanotechnology applications derive from the improved functionalities of the nano-sized materials, which exhibit different physical, chemical and biological properties when compared with those at the macro scale. Nanotechnology enables the development of a new generation of innovative materials, products and processes with a large enforcement in several industries such as electronics, engineering, medicine, agriculture, cosmetics and food (Augustin and Sanguansri, 2009). The study of bionanosystems as vehicles of biological and functional compounds has been of great interest for pharmaceutical and food applications (Cerqueira et al., 2014; Ramos et al., 2015).

In the 21st century there are several diseases affecting human wellbeing, which motivates science and technology professionals to join efforts and redirect their knowledge and activity to develop new strategies to address these public concerns, while facing the consumer's need, in order to contribute to a better global aging and life quality. Diabetes, cardiovascular diseases and gastrointestinal (GI) disorders are among the sundry diseases in which the food industry has significant impact and is increasingly focused in find suitable solutions (Cerqueira et al., 2014). One of the possible ways to struggle this issue is the consumption of bioactive compounds as nutraceuticals, such as vitamins, antioxidants, antimicrobials, and pre- or probiotics (Chen et al., 2014). Nutraceuticals are products derived from food sources with high nutritional value that provide health benefits, depending on their dosage and bioavailability. However, the nature of these compounds (e.g., poor water solubility, low stability), in their vast majority, may limit their bioavailability and therefore their application in food industry (Cerqueira et al., 2014). These limitations lead researchers to design and apply novel and more efficient delivery systems in order to address these challenges. One of the major concerns in terms of the use of nanostructures for food applications is the replacement of non-food-grade materials by bio-based, biodegradable and generally recognized as safe (GRAS) materials (Kwak, 2014). Regarding the nutraceutical characteristics, one the most recent and interesting vehicles used for their protection and controlled release in food matrices are the whey protein nanostructured systems (Cerqueira et al., 2014; Ramos et al., 2015).

This study is focused on the use of a Lactoferrin (LF) whey protein nanohydrogels, as encapsulating agent, for curcumin, used as nutraceutical model. The release kinetics of curcumin from LF nanohydrogels when incorporated into food simulants (i.e., hydrophilic medium ethanol 10 % and lipophilic medium ethanol 50 %), were also evaluated, as well as the behaviour of the LF nanohydrogels and curcumin in real food matrices (i.e., gelatine and olive oil).

2.2. Bio-based materials

2.2.1. Polysaccharides

These bio-based materials are polymeric carbohydrate macromolecules formed by the association of long chains of monosaccharides units. Polysaccharides such as chitosan, alginates, carragenates and pectins have a wide range of molecular weight which depends on the number of units of monosaccharides that bind to each other (Shen and Patel, 2008). They can be hydrolysed in smaller polysaccharides, as well as in disaccharides or monosaccharides through the action of certain enzymes (Liu et al., 2008). Polysaccharides are among the most renewable and abundant resources in nature and thus, they have low cost in their processing (Mizrahy and Peer, 2012). Particularly, most of natural polysaccharides have hydrophilic groups such as hydroxyl, carboxyl and amino groups, which could form non-covalent bonds with biological tissues, thus contributing to their bioadhesive properties (Lee et al., 2000). An experimental study refers to dextrin nanogel as an effective nanocarrier for lipophilic curcumin, by increasing its water solubility, thus improving its stability and controlling its release profile (Gonçalves et al., 2012). All these features endow polysaccharides a promising future as biomaterials in several fields.

2.2.2. Lipids

Lipids are a large and diverse group of naturally occurring organic compounds that are related by their insolubility in water and solubility in nonpolar organic solvents (Fahy et al., 2009). Depending on their structure, there are several lipids such as fats, waxes, sterols, monoglycerides, diglycerides, triglycerides and phospholipids. Researchers may largely define lipids as hydrophobic or amphiphilic molecules, where the amphiphilic nature of some lipids allows them to form structures such as vesicles, multilamellar or unilamellar liposomes, and membranes in an aqueous environment. The main biological functions of lipids include storing energy, signalling, and acting

as structural components of cell membranes (Fahy et al., 2009). Lipids have applications in the cosmetic, pharmaceutical and food industries, as well as in the nanotechnology field. In this context, they already have remarkable advances as delivery platforms (Mashaghi et al., 2013).

2.2.3. Proteins

Proteins are biological macromolecules, consisting of one or more long chains of amino acid residues. Their function is dictated by an amino acid sequence, which specifies a three-dimensional (3-D) structure that is a prerequisite for protein function, determining their activity (Dunker et al., 2002). The sequence of amino acid residues in a protein is defined by the sequence of a gene, which is encoded in the genetic code (Floudas et al., 2006). Like other biomolecules, such as polysaccharides and nucleic acids, proteins are essential parts of organisms and participate in practically every process within cells. Many proteins are enzymes that catalyse biochemical reactions, being considered vital molecules for metabolism (Dunker et al., 2002). Proteins have also structural or mechanical functions, such as actin and myosin in muscle and keratin and tubulin in the cytoskeleton, which form a system of scaffolding that maintains cell shape. They have also important biological properties, in particular, in cell signalling, immune responses, cell adhesion and cell cycle (Pennington et al., 1997). Proteins can associate to form stable protein complexes and therefore, work together to perform a particular function (Floudas et al., 2006). Several techniques such as ultracentrifugation, precipitation, electrophoresis, chromatography and others are used to obtain purified proteins. Within the usage of nanotechnology techniques, proteins can be used to adopt or form novel structures at nanoscale, which may display improved or new functionalities that can be very helpful to address many current health issues. In fact, there are several types of proteins with such capabilities, which can be isolated and purified from various sources.

Whey protein, a by-product of cheese-manufacture process, provide substantial amounts of the essential amino acids that are needed to carry out the functions that proteins perform in the body. Additionally, several whey proteins present interesting properties which allow their manipulation at various size scales, as well as their application in food, pharmaceutic and dermo cosmetic industry. A brief description of whey proteins was accomplished in section 2.3.

2.2.4. Different combinations of bio-based materials

The ability to combine different biomaterials brings out multi-functional systems that can be applied in different applications with requirements related to the different properties of those materials. It is required a proper combination of the different materials (e.g., polysaccharides, proteins and lipids) to allow the development of the nano-delivery systems with improved mechanical, stability and barrier resistance, as well as with higher encapsulation efficiency, stability and bioavailability of nutraceuticals (Souza et al., 2017). For instance, in 2015, Arroyo-maya and Mcclements, reported the combination of polysaccharides and proteins as a suitable solution for the development of efficient oral delivery systems for anthocyanins (Arroyo-maya and Mcclements, 2015). Polysaccharides such as alginate, chitosan and pullulan exhibit high adhesiveness to the intestinal mucosal surface and possess high stability under severe gastric conditions (Mizrahy and Peer, 2012). On the other hand, proteins have a high nutritional value and the ability to form gels (Chen et al., 2006). Table 1 presents some examples of bio-based nanosystems, regarding their main techniques and materials, bioactive compounds, size and encapsulation efficiency (%).

Table 1. Examples of bio-nanosystems: principal techniques and materials, encapsulated functional ingredients, size and encapsulation efficiency (%). (Adapted from Souza et al., 2017)

Bio-based material	**Encapsulating material**	**Bioactive compound**	**Encapsulation technique**	**Size**	**Encapsulation efficiency (%)**	**Reference**
Polysaccharide-based material	Zein starch	Curcumin	Antisolvent precipitation	153 nm	11.7	(Zou et al., 2015)
	Hydroxypropyl cellulose	Lycopene	Spray drying	NA	29.7	(Rocha et al., 2011)
Milk protein-based material	Whey protein isolate hydrogels	Bilberry extract	Emulsion	NA	NA	(Betz et al., 2012)
	β-lactoglobulin	Thiosulfinate allicin	Freeze drying and spray drying	NA	NA	(Wilde et al., 2016)
Lipid-based material	Liquid oil (Octyloctanoat) and solid lipid (Precirol)	Vitamin A	Hot homogenization	74–779 nm	98.5	(Pezeshki et al., 2014)
Combination of bio-based materials	Maltodextrin-Arabic gum	Barberry (*Berberis vulgaris*) extract	spray drying	NA	96.2	(Mahdavi et al., 2016)

Note: NA: Information not available.

2.3. Whey proteins

Whey proteins are globular molecules isolated from whey, which consists in a turbid yellowish liquid produced as a by-product of cheese manufacture. These proteins are one of the primary proteins found in dairy products and they are referred to be as one of the most widespread additives in food (Acevedo-fani et al., 2017). Whey proteins typically comes in four major forms: concentrate (WPC), isolate (WPI), hydrolysate (WPH) and native whey, where the WPI and WPC forms, are now included in commercial whey protein products (Ramos et al., 2015). As presented in table 2, the major whey protein fraction is mostly constituted by β-lactoglobulin (β-Lg), α-lactalbumin (α-La), immunoglobulin (IG) and bovine serum albumin (BSA, which represent 50 %, 17 %, 10 % and 6 %, respectively. As minor components of whey proteins, the lactoperoxidase (LP), proteose peptone (PP) and LF (lactoferrin) represent almost 17 % of this fraction (Ramos et al., 2015). In Table 2 are represented the general physicochemical properties of the main whey proteins.

2.3.1. β-Lactoglobulin

β-Lactoglobulin (β-Lg) is the major protein fraction of bovine whey serum and its principal gelling agent (Brownlow et al., 1997). It is a relatively small globular protein that can bind to small hydrophobic molecules such as retinol, fatty acids, triacylglycerols, aromatic compounds, vitamin D, cholesterol, palmitic acid, and calcium, thus suggesting an important role in the transport of these molecules. β-Lg has two disulphide bridges, and a free thiol group (SH). These characteristics and others shown in Table 2, provide a potential for intermolecular and intramolecular disulphide link interchange during conformational changes associated with pH alterations, heat, or pressure treatment (Gunasekaran et al., 2005). Its ability to form gels as well as its high nutritional and functional value endows β-Lg as an ingredient of high quality with application in pharmaceutical, food and beverage industry (Acevedo-fani et al., 2017).

2.3.2. α-Lactalbumin

α-Lactalbumin (α-La) is a small and globular protein which is able to bind hydrophobic ligands such as retinol (Livney, 2010), hydrophobic column chromatography phases, hydrophobic peptides, melittin of bee venom (Sa, 2006) and oleic acid (Gustafsson et al., 2005; Kehoe and Brodkorb, 2012). α-La is rich in cysteine which is an essential coenzyme for the biosynthesis of

lactose. Moreover, it contributes to reducing the risk of incidence of some cancers (e.g., breast and colon cancer) and has an impact in the treatment of the chronic stress-induced disease, which affects the cognitive performance (Acevedo-fani et al., 2017).

2.3.3. Immunoglobulin

Immunoglobulin (Ig) is a protein that is present in the serum and physiological fluids of all mammals and is produced by β-lymphocytes. Among other functions, Ig plays a crucial role in the immune function of mucous membranes and has antibacterial and antifungal activity. This protein can act as receptors attaching to surfaces, while others function as antibodies that are released in the blood and lymph (Fagarasan and Honjo, 2003).

2.3.4. Bovine serum albumin

Bovine serum albumin (BSA) is a small, stable, moderately non-reactive protein that can interact with lipoproteins, participating in energy production. It is used as an enzyme stabilizer during purification or for the dilution of restriction endonucleases and nucleic acid modification enzymes (Kang et al., 2009). BSA can bind to fatty acids, free fatty acids and flavour compounds. Furthermore, these proteins showed antioxidant, antimutagenic and anticarcinogenic activity (Hernández-ledesma et al., 2011; Madureira et al., 2010).

2.3.5. Lactoferrin

LF is a globular single-chain glycoprotein of the transferrin family folded into two globular lobules, which is present in several fluids such as milk, saliva, tears and nasal secretion. As one of the components of the immune system of the body, LF has great biological properties such as antibacterial, antiviral, immunomodulatory and iron binding capacity (Lonnerdal and Iyer, 1995; Brock, 2002). It has been reported the formation of nanohydrogels, by combining LF with glycomacropeptides (GMPs), and LF-based nanoparticles as vehicle for iron, both for food and pharmaceutical applications (Bourbon et al., 2015; Martins et al., 2016). LF high nutritional and functional value, as well as its ability to form gels, endows this protein as a high-quality ingredient with application in pharmaceutical, cosmetics, food, and beverage industry.

2.3.6. Lactoperoxidase

Lactoperoxidase (LP) is an enzyme from the family of peroxidases and it is secreted from mammary, salivary and other mucosal glands. This protein provides protection against microorganisms and fungus, and it has immunomodulatory activity (Al-baarri et al., 2011). LP is known for its ability to control microorganism growth in milk from lactating animals and additionally, it plays a significant function in oral health care that is associated to gingivitis and oral irritation. Furthermore, LP has been reported as an anti-tumour and anti-viral agent (Acevedo-fani et al., 2017).

Table 2. Representation of the main proteins in bovine whey, relative concentration (g L^{-1}), molecular weight (Mw), isoelectric point (pI), temperature of denaturation (Td) and number of amino acid residues (Adapted from Ramos et al., 2015).

Whey proteins	**Concentration (g L^{-1})**	**Mw (kDa)**	**pI**	**Td (°C)**	**Number of amino acid residues**
β-Lactoglobulin	3.5	18.3	5.2	71.9	162
α-Lactalbumin	1.2	14.2	4.8	64.3	123
Immunoglobulins	0.7	150-900	5.5-6.8	–	–
Bovine serum Albumin	0.4	66.4	4.7-4.9	72.0-74.0	583
Proteose peptones	≥1	<12	3.3-3.7	–	–
Lactoferrin	0.02–0.35	80.0	8.0-8.5	63.0 and 90.0	700
Lactoperoxidase	0.01–0.03	78.5	9.8	70.0	612

Note: (–) Variable values.

2.4. Whey protein nanostructures

There are many examples of engineered bio-based nanomaterials that can be produced from food-approved components and which are likely to be metabolized during digestion (e.g., proteins,

starch and lipids). Food proteins can be fabricated into novel nanoparticles that have potential applications in food industry. Proteins are known to be versatile structures since they're capable to adopt different forms, which depend on some variables regarding their physical, chemical and biological properties. For example, by altering the pH, it is possible to alter the nature of the proteins' aggregation process. By investigating such phenomena, becomes possible to design and produce novel fibrous or tubular structures (Sozer and Kokini, 2009; Livney, 2010). These methodologies allow to use these protein structures in texture modification, encapsulation and for moderating protein digestion with a possible influence in allergenicity (Morris, 2011). Among the whey protein nanostructures, the most commonly used for pharmaceutical and food purposes includes the nanohydrogels, nanofibrils and nanotubes (Ramos et al., 2015), as detailed below.

2.4.1 Nanohydrogels

Protein nanohydrogels are characterized by their three-dimensional, hydrophilic nano-sized networks that provide a swelling capability to these protein gels. This characteristic allow nanohydrogels to swell in water and hold large amounts of water while sustaining the network structure due to the presence of covalent and noncovalent bonds, or physical crosslinks (Chen et al., 2006; Gyarmati et al., 2013). The reduced size of nanohydrogels usually comprised from 50 to 300 nm coupled with their large surface area, and an interior network for incorporation of nutraceuticals enables: (i) encapsulation and controlled release of bioactive compounds; (ii) improved solubility and bioavailability of bioactive compounds; (iii) target deliver nutraceuticals in the associated tissues (e.g., reducing the GI mucosa irritation caused by continuous contact with some nutraceuticals) and/or protecting them against degradation and undesirable chemical reactions; and (iv) stability of such compounds in the GI tract (Ramos et al., 2015). Several techniques reported in literature are used to produce protein nanohydrogels with some food grade materials. Nonetheless, WPI such as β-Lg, are the most commonly used bio-based materials for this purpose, while gelation, which consists in protein unfolding and aggregation processes followed by the formation of three-dimensional network, is the main technique (Montejano et al., 2002). Protein nanohydrogels are also called 'smart' hydrogels due to their sensitivity to environmental conditions such as temperature, pH, light and solvent composition, that can induce different responses as function of pre-determined stimuli (Qiu and Park, 2012). These features make protein hydrogels, tuneable and desired nanostructures for use in the food industry (Maltais et al., 2009).

2.4.2. Nanofibrils

Nanofibrils are semi-flexible structures with persistence lengths larger than 1 μm, and an average diameter between 4 and 10 nm (Loveday et al., 2012). The formation of whey protein nanofibrils occurs when the whey proteins forms aggregates that are stabilized by a long range and weak electrostatic interactions. Protein nanofibrils can embroil to form nanohydrogels at relatively low protein concentrations (Ramos et al., 2015). Recent research referred salt addition, mild heating and hydrolysis as some needed strategies to produce α-La or BSA nanofibrils (Goers et al., 2002; Veerman et al., 2003; Loveday et al., 2010). It has been referred that these structures may potentially act as thickeners, gelling, emulsifying or foaming ingredients in foods, while also increasing their nutritional value (Ramos et al., 2015).

2.4.3. Nanotubes

Nanotubes are nanometre-scale tube-like structures usually exhibiting an outer diameter of ca. 20 nm, a cavity diameter of ca. 7–8 nm, and several hundreds of nanometres (or even micrometres) long with the ability to involve other nanoparticles (Ramos et al., 2015). Whey protein nanotubes can be produced by partial hydrolysis of α-La, catalysed by a serine endoprotease from *Bacillus licheniformis* in the presence of divalent cations, which promotes the formation of salt-bridges between two deionized carboxylic groups (Graveland-bikker et al., 2004; Ipsen and Otte, 2007). Furthermore, whey protein nanotubes show advantages over other protein structures, since their open ends, on both sides of the tubes, may provide a more efficient delivery and controlled release of nutraceuticals (Ipsen and Otte, 2007; Sadeghi et al., 2013).

2.5. Bioactive compounds and nutraceuticals

Bioactive compounds such as vitamins, antioxidants, antimicrobials and polyphenols, are naturally presented in food and provide health benefits beyond the basic nutritional value of the product. These compounds are being extensively studied to evaluate their effect on health aiming to prevent several diseases, contributing to consumer wellbeing (Li-chan, 2015). Bioactive compounds are also referred to as nutraceuticals due to their existence in human diet and biological activity. Nutraceuticals can be proteins, nutrients, dietary supplements, genetically engineered food and processed foods, such as cereals, soups and beverages (Biesalski et al., 2009). During the food

chain procedures (i.e., processing, transportation and storage), nutraceuticals are susceptible to physical, chemical and enzymatic degradation, which should be overcome. Therefore, bioactive substances should not be added directly (in their pure state) to food matrices. For that reason, it is necessary to encapsulate them in order to preserve their bioavailability and avoid undesirable effects (Souza et al., 2017). There are several different types of bioactive compounds, which some of them are described below.

2.5.1. Vitamins

Vitamins are organic compounds and, as a vital nutrient required for organisms, they play an essential role in growth, development and normal maintenance of the human body (Patel et al., 2015). Only vitamin D and B_3 can be naturally produced by the human body, being the remaining vitamins obtained through the diet. Regarding their solubility, these nutraceuticals can be divided into two categories: (i) hydrophilic (i.e., vitamin B1, B2, B3, B5, B6, B7, B9, B12 and vitamin C); and (ii) lipophilic (i.e., vitamin A, D, E and K) (Souza et al., 2017). The deficiencies in vitamin uptake could lead to the development of certain diseases. Although the administration of vitamins through supplements and conventional nutraceuticals seemed to be an alternative for this issue, later it demonstrated to be inefficient, due to their susceptibility to degradation during processing and storage, until the moment of their absorption in the GI tract. The encapsulation of these compounds through the use of food-grade nanostructures proved to be one of the best alternatives for their protection and proper release (Taib et al., 2016).

2.5.2. Antioxidants

Antioxidants are molecules capable of slowing or preventing oxidative damage, a process caused by substances called free radicals and nitrogen species, which can lead to DNA damage and cell dysfunction, thus resulting on the appearance of several diseases, such as heart disorders, diabetes, tumours and so forth. The role of antioxidants is to block oxidation reactions and provide protection to membranes and other parts of cells (Kumar et al., 2013; Quirós-sauceda et al., 2014). Phytochemicals represent a large group of plant-derived compounds, including polyphenols, flavonoids, isoflavones and carotenoids. They are quoted as antioxidant and anti-inflammatory agents, hence providing many health benefits. When conventionally incorporated in food products, phytochemicals present undesired sensory properties (e.g., off-flavours and odours). Therefore,

they need to be encapsulated in order to mask their unpleasant characteristics, permitting their use at higher concentrations without causing adverse effects for the consumers (Shome et al., 2016).

Polyphenols constitute a large family of varied substances which can act as secondary metabolites. These compounds are commonly present in vascular plants and can be grouped together in several classes. Polyphenolic compounds are able to scavenge radical oxygen species and possess anti-inflammatory properties. These abilities make polyphenols interesting compounds for pharmaceutical, cosmetic applications.

Curcumin is a yellowish polyphenol from Turmeric spice (*Curcuma Longa*) and has shown multiple health benefits due to its anti-inflammatory and antioxidant potential. However, this nutraceutical is sparingly soluble in aqueous solutions due to the presence of a large number of aromatic rings, and also presents low bioavailability (Hazra et al., 2014).

Curcumin is already used as a flavouring and colouring agent in the food industry (Munin and Edwards-lévy, 2011). However, several research areas are still making an effort to study curcumin health benefits and its application in pharmaceutical and food industries.

2.5.3. Antimicrobials

Antimicrobials are chemical substances with the ability to inhibit microorganisms' growth, thus providing antibacterial and antifungal activity. Such compounds display an important role in controlling the development and proliferation of pathogenic microorganisms in food products. Antimicrobials can be enzymes (e.g., lactoperoxidase), polysaccharides (e.g., starch), bacteriocins (e.g., colicins), herbs, spices, essential oils (e.g., terpenes), alcohols, ketones, phenols, acids, aldehydes and esters (Tajkarimi et al., 2010). Among other agents, essential oils (e.g., lemon oil, terpineol, Melissa oil and fish oil) are envisaged as one the most interesting nutraceuticals by food industry, due to their significant antimicrobial activity (Calo et al., 2015). However, they are limited compounds because of their hydrophobicity, high volatility and reactivity, and undesirable aroma. For that reason, their encapsulation is being studied as a feasible solution to overcome these issues (Quirós-sauceda et al., 2014).

2.5.4. Other nutraceuticals

Enzymes are considered nutraceuticals when its function is to accelerate chemical reactions. Their applicability in food industry is well known, but they present relatively high cost production (Davidov-pardo et al., 2015). Enzymes can be inactivated when subjected to adverse environmental conditions. Therefore, their encapsulation may appear as suitable solution to avoid undesired reactions as being reported in several studies. For instance, a study has shown that the encapsulation of enzymes in food gum gels for accelerated cheese ripening is feasible (Kailasapathy and Lam, 2005). Besides enzymes used in food industry, probiotics and prebiotics, minerals and natural flavourings are also considered nutraceuticals, depending on their purpose usage. There are many studies reviewing the encapsulation of such compounds (Quirós-sauceda et al., 2014; Dubey and Windhab, 2013).

2.6. Encapsulation techniques

The encapsulation of nutraceuticals can be performed by several techniques and their selection depends on the nature of the bioactive compound and of the nanostructure, as well as on the properties of the nanostructure to be designed (Desai and Park, 2005). Additionally, there are two inherent variables that should be considered, the encapsulation efficiency and the cost production. Encapsulation process can be performed by two approaches which are, the “bottom-up” and the “top-down”. Bottom-up approach is when the structure is created from smaller building blocks (atom-by-atom or molecule-by-molecule). On the other hand, top-down approach is when the structure is cut out from a bigger piece "manually" or by self-structuring process (Tavares et al., 2014). There are a vast diversity in the encapsulation techniques, which shows that the production of micro- and nanostructures for food industry can be performed in different ways, depending on the intended functionality (Ezhilarasi et al., 2013). However, taking into account the content of this study, it will be given particularly focus on thermal gelation as encapsulation technique and freeze-drying as dehydration method.

2.6.1. Thermal gelation

Thermal gelation of proteins is usually initiated by an unfolding process of the native proteins through the action of heating in function of time. Then, the primary aggregation process which

occurs through covalent (e.g. disulfide bridges) and noncovalent (e.g. hydrogen bonds and hydrophobic interactions) bonds is promoted, followed by secondary aggregation consisting on the aggregation of protein primary-aggregates. Finally, a three-dimensional network is formed enabling this protein gels to swell and to entrap large amounts of water (Ramos et al., 2015). Depending on the concentration, pH, temperature, ionic strength and electric fields, protein gels can adopt several different nanostructures such as nanohydrogels, nanotubes and nanofibrils (Rubinstein and Colby, 2003). The incorporation of nutraceuticals into these structures can be accomplished through the addition of such compounds before, after and during gelation process, depending on the materials and application.

2.6.2. Freeze-drying

Freeze drying, commonly known as lyophilisation, is a technique based on the dehydration by sublimation of a frozen product. It consists in two steps: (a) rapid freezing of the product and (b) sublimation of the ice under vacuum (Ray et al., 2017). An encapsulation process can be performed by lyophilizing an emulsion of the core material with an encapsulating agent. This method generates products of excellent quality, since it minimizes the changes associated with high temperatures. In fact a study demonstrated that lyophilisation encapsulation method resulted in less degradation of β-carotene (Desobry et al., 1997).

2.7. Food matrices

2.7.1. Food simulants

According to the Commission Regulation (EU) No 10/2011 of 14 January 2011 on plastic materials and articles intended to come into contact with food, it is compiled in Annex III a list of regulated food simulants (also presented in Table 3) for plastic materials and articles not yet in contact with food (EC, 2011). These simulants are used to mimic the conditions of real food matrices, thus allowing to study the impact of food environmental conditions on controlled release systems.

Table 3. List of available food simulants regarding their composition and applications (Adapted from European Parliament and Council).

Food simulant	Composition	Application
A	Ethanol 10 % (v/v)	Hydrophilic food products
B	Acetic acid 3 % (v/v)	Hydrophilic and acidic food products (pH < 4.5)
C	Ethanol 20 % (v/v)	Hydrophilic and alcoholic foods products (≤ 20 % alcohol)
D1	Ethanol 50 % (v/v)	Lipophilic, alcoholic (≥ 20 % alcohol) food products and oil-in-water emulsions
D2	Vegetable oil	Lipophilic food products and superficial fats
E	Poly (2,6-diphenyl-p-phenylene oxide), particle size of 60–80 mesh, pore size 200 nm	Dry food products

2.7.2. Real food matrices

Food products can have a detrimental, neutral or protective effect over the delivery systems containing nutraceuticals. Generally, food additives may include different types of sugars, salts, aromas, natural and/or artificial flavourings, among others. They can interact with delivery systems, decreasing their bioavailability and thus, the bioactivity of the nutraceuticals may be compromised (Vos et al., 2010). There are several studies evaluating the incorporation of controlled delivery systems in distinct food matrices such as yogurt (Pando et al., 2015), fruit juice (Nualkaekul et al., 2013), cheese (Hernández-ledesma et al., 2011), among others. A recent study demonstrated that resveratrol entrapped into niosomes is a suitable additive in regular yogurts (Pando et al., 2015). Nualkaekul et al., 2013 infered that alginate and pectin beads coated with chitosan or gelatine improved dramatically the survival of *L. plantarum* and *B. longum* in pomegranate and cranberry juice (Nualkaekul et al., 2013). In this study, a gelatine and olive oil were used as hydrophilic and lipophilic food matrices, respectively. These food matrices were chosen due to their simplicity and transparency, which may facilitate their characterization at a

spectroscopic level. In addition, both food products are usually stored at different environmental conditions such as 4 °C and 25 °C for gelatine and olive oil, respectively. However, since solubility was not achieved when nanohydrogels were incorporated into the olive oil food matrix, the methodology and respective results are not shown. Therefore, only the data regarding the tests performed on gelatine are presented and discussed in the following chapters.

2.8. Techniques used during this study

2.8.1. Dynamic light scattering

Dynamic light scattering (DLS) is a non-invasive, well-established technique for measuring the size and size distribution of molecules and particles typically in the submicron region. A laser (He-Ne) illuminates the solution and light is scattered at different intensities, due to the Brownian motion of particles or molecules in suspension (Schmitz and Phillies, 1991). This technique analyses intensity fluctuations by means of photon auto-correlation function and hence, it yields the particle size using the Stokes-Einstein relationship. Typical applications of dynamic light scattering includes the characterization of proteins, polymers, micelles, vesicles, carbohydrates, nanoparticles, biological cells and gels that have been dispersed or dissolved in a liquid (Sabareesh et al., 2006).

2.8.2. Ultraviolet-visible spectroscopy

Ultraviolet–visible (UV–Vis) spectroscopy refers to the absorption spectroscopy or reflectance spectroscopy in the ultraviolet-visible spectral region. Absorption of visible and ultraviolet radiation is associated with excitation of electrons, in both atoms and molecules, from lower to higher energy levels. Only light with the precise amount of energy can cause transitions from one level to another and thus, it will be absorbed (Weckhuysen, 2004). The absorption or reflectance in the visible range affects directly the perceived colour of the chemicals involved. Absorption spectroscopy measures transitions from the ground state to the excited state, while fluorescence deals with transitions from the excited state to the ground state. Therefore, UV–Vis spectroscopy is complementary to fluorescence spectroscopy (Lakowicz, 2006).

2.8.3. Fluorescence spectroscopy

Fluorescence spectroscopy is a type of electromagnetic spectroscopy that analyses fluorescence from a sample. It involves the use of a beam of light, usually ultraviolet light, that excites the electrons in molecules of certain compounds and causes them to emit light. In the special case of single molecule fluorescence spectroscopy, the intensity fluctuations from the emitted light are measured from either single fluorophores, or pairs of fluorophores (Weiss, 1999). Fluorescence spectroscopy presents a variety of interesting techniques, such as fluorescence resonance energy transfer (FRET), lifetime fluorescence, synchronous fluorescence, among others (Lakowicz, 2006). In this specific field, fluorescence analysis may be a valuable tool to monitor protein conformational changes, binding phenomena among other events (St et al., 2012).

2.8.4. Circular dichroism spectrometry

Circular dichroism (CD) involves circularly polarized light by means of the differential absorption of left- and right-handed light. CD signals are exhibited in the absorption bands of optically active chiral molecules and thus, spectral bands are easily assigned to distinct structural characteristics of a biomolecule (Greenfield, 2006). CD is a valuable tool for the evaluation of the secondary structure, conformational changes and binding properties of proteins. As a result, different structural elements acquire a characteristic CD spectrum (Kelly et al., 2005).

2.8.5. Fourier transform infrared spectroscopy

Fourier transform infrared (FTIR) spectroscopy is one of the main vibrational spectroscopic techniques with potential to be applied in biological, chemical, biomedical and even in clinical fields. Infrared spectrum can be used as a fingerprint for the identification of numerous molecules (Movasaghi et al., 2008). FTIR analysis can be carried out by comparing the spectrum from an unknown specie or molecule with previously recorded reference spectra. In vibrational spectra, the spectral bands are molecule specific and can provide accurate information about the biochemical composition (Talari et al. 2017). Additionally, FTIR spectra also provide valuable information at a molecular level, allowing the determination of functional groups, bonding types and molecular conformations. Spectral data is most often used, as qualitative analysis, in the percentage

transmittance format (%, *T*), which has a logarithmic relationship ($-\log_{10}$) with respect to the absorbance (Abs) (Coates, 2000).

2.8.6. Transmission electron microscopy

In transmission electron microscopy (TEM), a thin specimen is irradiated with an electron beam of uniform current density, to form an image (Reimer, 1993). The specimen is usually a thin section less than 100 nm thick or a suspension on a grid. Transmission electron microscopes are capable of imaging at a significantly higher resolution than light microscopes. This enables the instrument to capture fine detail, even at nanometre scale. TEM is a major analytical method in the physical, chemical and biological sciences and it finds application in cancer research, virology and materials science, as well as in pollution, nanotechnology and semiconductor researches (Hanker et al., 1987)

2.8.7. Native electrophoresis

Gel electrophoresis is a valuable method for separation and analysis of macromolecules such as DNA, RNA, proteins and their fragments. When applied an electric field, molecules may move through a gel made of agarose or polyacrylamide (Blackshear, 1984). This technique enables macromolecules to sort in function of their size and charge. It is applied an electric field of a negative charge, which pushes the molecules through the gel, and a positive charge that pulls the molecules through the gel. The molecules are dispensed into a well in the gel material, which is placed in an electrophoresis chamber and connected to a power source. When the electric current is applied, the larger molecules move slowly through the gel while the smaller molecules move faster. The different sized molecules form distinct bands on the gel (Magdeldin et al. 2014).

CHAPTER 3 – MATERIALS AND METHODS

3.1. Materials

Purified bovine lactoferrin (LF) powder, composed by 96 % protein, 0.5 % ash, 3.5 % moisture and 0.012 % iron (data supplied by the manufacturer), was purchased from DMV International (USA). Hydrochloric acid (HCl) (37–38.0 % purity), 8-Anilinonaphthalene-1-sulfonic acid (ANS) and curcumin powder with purity > 65 % (HPLC grade) were purchased from Sigma–Aldrich Chemical Co. Ltd. (Darmstadt, Germany). Pure ethanol (99.5 % purity) and sodium hydroxide (pellets) were obtained from JMGS (Portugal). Unflavoured gelatine (powder) was commercially purchased in a local supermarket (Braga, Portugal).

3.2. Development of nanohydrogels

3.2.1. Preparation of LF solutions

Nanohydrogels preparation was based in the methodology used by other authors (Bengoechea et al., 2011; Martins et al., 2016), with some modifications described as follows. Briefly, a weighted amount of LF was dissolved in distilled water at 25 °C and stirred (300 rpm) for 1 h until reach a 0.2 % (w/v) concentration. The pH value of LF solution was adjusted to 7.0, with 0.1 mol L^{-1} of sodium hydroxide (NaOH). LF aqueous solution was submitted to a thermal treatment in which it was heated at 75 °C for 0, 5, 10, 15 and 20 min in a water bath (closed system), to promote the formation of a monodisperse nanohydrogel solution. All the samples were made in triplicate and kept at room temperature (25 °C) for at least 30 min until further characterization.

3.2.2. Preparation of nanohydrogels incorporating curcumin

The determination of the association efficiency (AE) served as a measure to attain the higher possible amount of curcumin able to associate with LF nanohydrogels. Regarding the loading capacity (LC), this variable gives the percentage of the capacity that LF nanohydrogel has to load curcumin molecules in its net. Therefore, an experimental methodology (represented in Figure 1) was adopted and designed to obtain such valuable information. Initially, a range of concentrations between 66 and 1066 μg/mL from a curcumin stock solution (3000 μg/mL), previously dissolved in pure ethanol (EtOH) and stirred for 20 min, was prepared. In order to mix LF-curcumin solutions, approximately 750 μL from each of curcumin solutions were added to the corresponding LF solutions, until reach increasing curcumin concentrations between 10 and 120 μg/mL. The final

volume was fixed in 10 mL per solution composed by EtOH at a concentration of 7.5 %. Then, after 20 min of gentle stirring, LF-curcumin mixtures were finally heated at 75 °C in a water bath (closed system) during 10 min (solutions represented in Figure 2). The unbound curcumin was removed from the nanohydrogel solutions by centrifuging at 12 000 *g* for 20 min. The pellet composed by undissolved curcumin was thoroughly dissolved in pure ethanol and further analysed spectroscopically at 425 nm following the procedure described elsewhere (Bourbon et al., 2016). The AE was accessed by estimating the amount of free curcumin, using a calibration curve made in the same conditions of the solutions from the re-dissolved pellet. The resulting equation y=0.1305x-0.0109, R^2 = 0.9959, allowed the determination of concentration values required to apply in a standard AE equation (Eq 1).

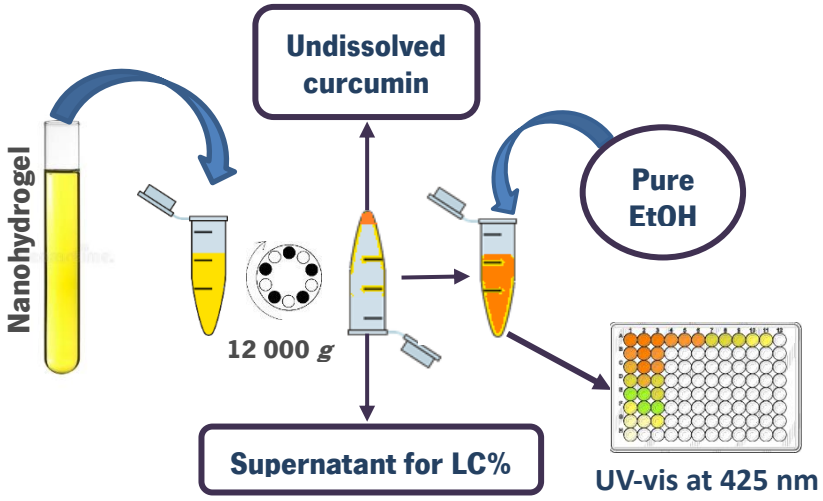

Figure 1. Schematic representation of curcumin quantification procedure for association efficiency (AE) determination.

$$AE\ \% = \frac{Total\ curcumin - Free\ curcumin}{Total\ curcumin} \times 100 \qquad \text{Eq 1}$$

$$LC\ \% = \frac{Total\ curcumin - Free\ curcumin}{Mass\ nanoparticles} \times 100 \qquad \text{Eq 2}$$

where *Total curcumin* represents the total amount of curcumin initially added to the LF nanohydrogel, *Free curcumin* is the amount of undissolved curcumin which did not associate with

nanohydrogels and *Mass nanoparticles* represents the total mass (µg) of nanoparticles after drying process.

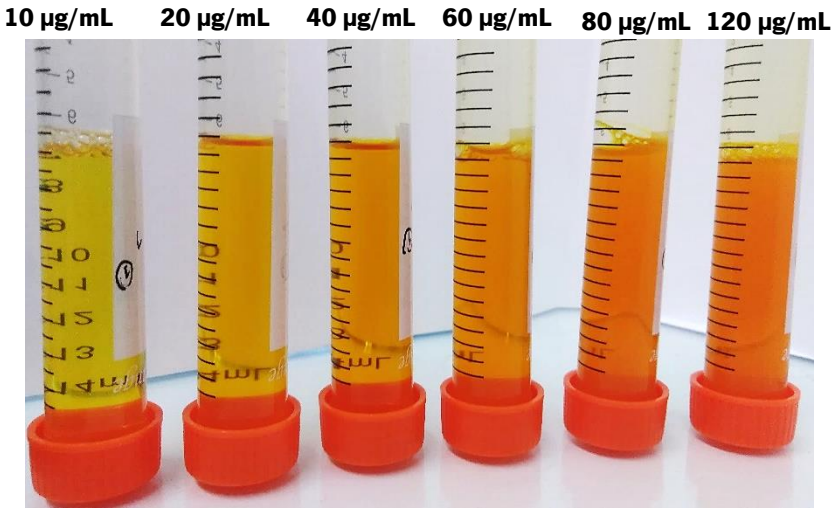

Figure 2. Representative image of LF-curcumin solutions in a range of concentrations between 10 and 120 µg/mL.

Concerning the LC determination, the removed supernatants were firstly dropped into new eppendorfs (previously dehydrated and weighted) and then, dried in an oven at 50 °C during 48 h. After this period, the eppendorfs containing the dried supernatants were rigorously weighted in an analytical balance (KERN ABJ-NM, Germany) with a precision of 0.0001 g, in order to determine nanoparticles mass, for further LC calculation (Eq 2). Finally, a calibration curve was prepared for LF quantification (presented in Figure 3) as a measure to show the absence of protein in the pellet previously obtained. Therefore, after centrifugation, the amount of lactoferrin in the supernatants was quantified and then, it was determined that 80 % from the total mass of LF was present in the supernatant.

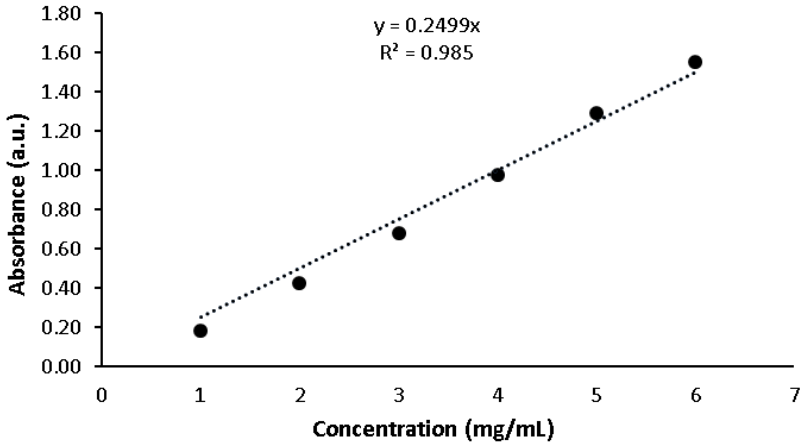

Figure 3. LF calibration curve for further quantification of the obtained supernatants.

3.3. LF-curcumin nanohydrogels dehydration

3.3.1. Freeze-Drying

LF and LF-curcumin solutions, prepared as described in section 3.2.1., were submitted to a freezing process starting with -20 °C during 24 h in a regular freezer, and followed by freezing until -80 °C in a laboratory grade freezer (Thermo Scientific, Massachusetts, USA). The freeze-drying experiment was conducted with a freeze-dryer (CHRIST - Alpha 1-4 LD plus, Germany), where solutions were placed for 5 days. After that period, the obtained nanohydrogels powders were stored at 20 °C in a desiccator until further utilization.

3.4. Nanohydrogels characterization

3.4.1. Dynamic light scattering

In order to validate the development of LF nanohydrogels with desired sizes, homogeneity and surface charge, the hydrodynamic diameter, polydispersity index (PdI) and ζ-potential of the LF nanoparticles were assessed. For this evaluation it was used a Dynamic Light Scattering (DLS) device (Zetasizer Nano ZS, Malvern Instruments, United Kingdom) equipped with a He-Ne laser at a wavelength of 633 nm. Size measurements were performed using patented NIBS (Non-Invasive Back Scatter) technology, with a backscatter angle of 173°. LF samples were placed in a regular polystyrene cuvette for size and PdI measurements, and in a disposable capillary cell for the ζ-potential determination. Initially this methodology was applied to monitor changes in size, PdI and ζ-potential of LF nanohydrogel in function of increasing holding times (0, 5, 10, 15 and 20 min) of heating at 75 °C. Furthermore, DLS technique was also used to assess the same parameters for LF nanohydrogel after its association with curcumin, as well as to validate the LF-curcumin nanohydrogel stability after lyophilisation process and after the release kinetics experiments. Finally, this technique was an important tool to monitor the system stability in storage conditions (refrigerated at 4 °C and room ambient at 25 °C) and after curcumin release into food simulants. All measurements were performed at 25 °C in triplicate. The results are shown as the average ± standard deviation of the experimental values.

3.4.2. Ultraviolet-visible spectrophotometer

In order to access LF solutions turbidity, an UV-vis measurement at 600 nm in a spectrophotometer (Jasco V-560, Japan) was performed. This test served to evaluate protein aggregation in function of holding time and also to validate the LF nanohydrogels development. Briefly, LF solutions (0.2 % at pH 7) were separately heated at 75 °C for increasing holding times (i.e., 0, 5, 10, 15, 20 min). Each of these solutions was placed in a quartz cuvette with a path length of 1.0 cm, a band width of 2.0 nm and a resolution of 1.0 nm. All samples were prepared and analysed in triplicate and the results are presented as the average ± standard deviation of the experimental values.

3.4.3. Intrinsic fluorescence

To monitor possible structural changes of LF protein when it is submitted to a thermal treatment with increasing holding times, fluorescence measurements were performed in a spectrofluorometer (Horiba Scientific, USA) equipped with a standard cell holder. LF solutions were heated at 75 °C for 0 to 20 min, where at every 5 min samples were collected in order to monitor changes in fluorescence intensity and to evaluate potential shift events. LF samples (0.2 % at pH 7) were placed into a quartz cuvette with a path length of 1.0 cm, and spectra were recorded with a resolution of 1.17 nm, 1 accumulation and an integration time of 0.1 s. The peaks were caught in the spectral range between 300 nm and 400 nm, with an excitation wavelength of 280 nm, where both tryptophan and tyrosine amino acids were excited at their maximum intensity. All samples were made in triplicate, where the spectra are presented as the average of the experimental values.

3.4.4. Extrinsic fluorescence

With the purpose of evaluate protein hydrophobicity and the occurrence of potential hydrophobic interactions between LF and curcumin, 8-Anilinonaphthalene-1-suLFonic acid (ANS) probe fluorescence measurements were performed in a spectrofluorometer (Horiba Scientific, USA) equipped with a standard cell holder. Samples were placed into a quartz cuvette with a path length of 1.0 cm and fluorescence records were made with a resolution of 1.17 nm, 1 accumulation and an integration time of 0.1 s. This methodology consists on the addition of ANS, a fluorescent probe with the particularity of emitting fluorescence when it is bind to protein hydrophobic residues (Lakowicz, 2006), to LF and LF-curcumin solutions. Then, ANS was excited at 370 nm. Firstly, LF

extrinsic fluorescence (exposure level of hydrophobic residues) was monitored after heating at 75 °C for 0 to 20 min, where at every 5 min LF samples (0.2 % at pH 7) were collected. Then, LF-curcumin solutions with increasing curcumin concentrations between 10 and 80 μg/mL were separately prepared and, the peaks were caught in the spectral range between 400 nm and 600 nm. As it was needed to record the fluorescence emission of the respective controls (LF-curcumin samples without ANS, excited at 280 nm and 425 nm), this experiment also served to evaluate fluorescence inhibition phenomena in function of increasing curcumin concentrations on LF-curcumin nanohydrogels. In these measurements, the acquired records did not present sufficient emission intensity in order to perform an adequate analysis and discussion of the results. This lack of intensity can be explained by excitation light attenuation and auto-absorption phenomena, which are usual occurrences within highly concentrated samples. Therefore, a triangular quartz cuvette, which enables the collection of emission records on the first millimetres of the sample was used and thus, it avoided the previous related phenomena. Samples were prepared in triplicate and spectra are given as the average of the experimental values.

3.4.5. Circular dichroism

To evaluate both the effect of increasing holding times during nanohydrogels development and the effect of curcumin association on LF secondary structure, circular dichroism (CD) measurements were carried out in a high-performance CD spectrometer J-1500m (Jasco, Italy). LF secondary structure was analysed in the far-UV (190 to 250 nm) of the CD spectra. Firstly, LF solutions (0.2 % at pH 7) were freshly prepared and diluted 10 times in distilled water for a proper signal acquisition. Then, 350 μL of each sample was carefully pipetted into CD cells with a path length of 0.1 cm. The second analysis, which consisted in the evaluation of the effect of curcumin incorporation on LF secondary structure, was performed in the same conditions above mentioned, considering the concentration of curcumin at 80 μg/mL. Finally, the effect of freeze-drying process on LF secondary structure was also assessed. CD spectra were recorded with a scanning speed of 50 nm/min, 1.0 nm resolution, 3 accumulations and a band width of 1.0 nm. The blank from the analysed solutions and the curcumin backgrounds were subtracted from the raw spectra, and the results are shown as the average of the experimental values as the samples were made in triplicate.

3.4.6. Fourier-transform infrared spectroscopy

In order to evaluate the interactions between curcumin and LF nanohydrogel matrix, as well as to confirm their association, Fourier transform infrared (FTIR) spectroscopy measurements were realized. LF and LF-curcumin nanohydrogel powders were prepared as described in section 3.3.1 and curcumin powder was used without any treatment. Samples were analysed in a Bruker IFS 66V spectrometer equipped with an Attenuated Total Reflection (ATR) module. FTIR-ATR spectra were acquired with a diamond crystal in the Golden Gate Single Reflection system (Specac) assembled to FTIR spectrometer, using non-polarized light at an incidence angle of 45°. Measurements were performed in vacuum in the wavenumber range between 550 cm^{-1} and 5000 cm^{-1} with a resolution of 4 cm^{-1}, by using a Globar source, a KBr beam-splitter and a DTGS detector with KBr window. In total, 32 scans were run for each measurement and the resulting spectra are given with previous background subtraction.

3.4.7. Fluorescence resonance energy transfer

Fluorescence resonance energy transfer (FRET) is a valuable tool for determining intramolecular distances between a specific donor-acceptor pair, where 50 % of the fluorescence energy of the donor (fluorophore) is transferred to the acceptor (chromophore) (Lakowicz, 2006). FRET occurrence analysis appears to be an interesting technique towards the acquirement of valuable information in terms of the pair's (acceptor ligands and donor fluorophores) binding distances, as well as their binding sites (Diarrassouba et al., 2013). Therefore, a FRET measurement was prepared consisting in the acquisition of both absorbance and fluorescence spectra of LF, curcumin and LF-curcumin solutions. This assay was carried out using a spectrofluorometer (Horiba Scientific, USA) and an UV-Vis spectrophotometer (Jasco V-560, Japan) for the fluorescence and absorption measurements, respectively. In both measurements, solutions were diluted until the acquisition of a reasonable signal, avoiding the overloading effect, where the initial LF-curcumin solutions were prepared in the same ratio described in section 3.2.2, at the maximum AE %. For the fluorescence spectra records, the excitation wavelengths were set at 280 nm and 425 nm for tryptophan (from LF) and curcumin, respectively. A triangular cuvette was used in this experiment for the fluorescence emission records, due to the same reasons described in section 3.4.4.

3.4.8. Transmission electron microscopy

To obtain valuable images of LF nanohydrogels, before and after its association with curcumin, transmission electron microscopy (TEM) was used. LF and LF-curcumin nanohydrogels were prepared as described in sections 3.2.1 and 3.2.2, respectively. TEM imaging was conducted on a Zeiss EM 902A (Thornwood, N.Y., USA) microscope at an accelerating voltage of 50 and 80 kV. A drop of sample dispersion was deposited onto a carbon support film mounted on a TEM copper grid (Quantifoil, Germany). The excess of solution was removed after 2 min using a filter paper, and the grid let for air-drying. The samples were then negatively stained with uranyl acetate (2 %, w/w) (Merck, Germany) for 15 s. The grid was finally air dried at room temperature (ca. 25 °C) before introducing it in the electron microscope. These conditions were used based in procedures usually adopted by our research group (Monteiro et al., 2016; Bourbon et al., 2015; Pinheiro et al., 2015).

3.4.9. Native electrophoresis

To evaluate both the denaturation of LF induced by thermal treatment and by freeze-drying process, before and after its association with curcumin, a native electrophoresis was performed. Mini-Protean TGX precast gels with 4-15 % of polyacrylamide (Bio-Rad) were used with Tris–glycine buffer, at a constant electric current of 10 mA in a Mini-Protean Tetra Cell (Bio-Rad, San Francisco) (Kügler et al., 1997). LF and LF-curcumin dehydrated samples were previously re-dissolved in the same volume of the respective original solutions (0.2 % at pH 7 heated at 75 °C for 10 min; curcumin at 80 μg/mL). All samples (10 μg/mL), previously diluted in distilled water, were mixed with 2x Laemmli sample buffer (RIORAD). Finally, an aliquot (15 μL) of each sample was loaded onto the same gel, and proteins were visualized with Coomassie Blue R-250 (Sigma, USA).

3.5. Evaluation of stability of nanohydrogels under storage conditions

LF-curcumin nanohydrogel stability was evaluated at 4 °C and 25 °C for 35 days of storage. Briefly, LF (control) and LF-curcumin solutions (0.2 % at pH 7, heated at 75 °C for 10 min; curcumin at 80 μg/mL) were prepared in day 0 and, for each of the analysis' periods, separately. Then, for storage at 25 °C, samples were kept at room temperature (25 °C) and protected from light. Further

on, for storage at 4 °C, the samples were stored in a regular fridge and protected from light, until further analysis.

The stability of nanohydrogels under storage was evaluated by measuring its size and PdI from day 0 to day 35. These parameters were assessed using DLS, as it was used in the previous analyses, above mentioned. All measurements were performed in triplicate. The results are presented as the average ± standard deviation of the experimental values.

3.6. Evaluation of curcumin release in food simulants

3.6.1. Release profiles

A release kinetics assay was performed with two different food simulants (i.e., hydrophilic and lipophilic media), at room temperature (25 °C) to access their behaviour under harsh storage conditions. The purpose of this test is to evaluate the curcumin release from LF nanohydrogels to food matrices using food simulants with different hydrophilicities. The first test was conducted with ethanol 10 % medium, corresponding to a hydrophilic food simulant (as shown in table 3 from chapter 1). The second one was carried out with ethanol 50 % medium, which corresponds to the lipophilic food simulant (presented in table 3 from chapter 1). LF-curcumin solutions were prepared in triplicate and, after separating the undissolved curcumin as described in section 3.2.2, 4 mL of each solution were placed into dialysis membranes with 10 kDa cut-off, which in turn those were emerged into three glass release reactors. Inside of each release reactor, the dialysis membranes were emerged into 50 mL of the selected media (according to the Commission Regulation EU No 10/2011) (EC, 2011). Distilled water at 25 °C was pumped with a heating pump-head, through all the release reactors, in order to maintain the temperature of the food simulant media. These experiments were also performed under a magnetic agitation at 250 rpm. Figure 4 represents the methodology adopted for this experiment. For both assays, samples taken from release reactors media from 0 min until a release stabilization, were spectrophotometrically analysed at 425 nm, using an UV-Vis spectrophotometer (Synergy HT, Bio-Tek, Winooski, USA). At each time that an amount of solution was taken, the same volume of the respective medium was placed into the release reactors as a method to avoid variation on the concentration of the released curcumin. All measurements were performed in triplicate and the results are given as the average ± standard deviation of the experimental values.

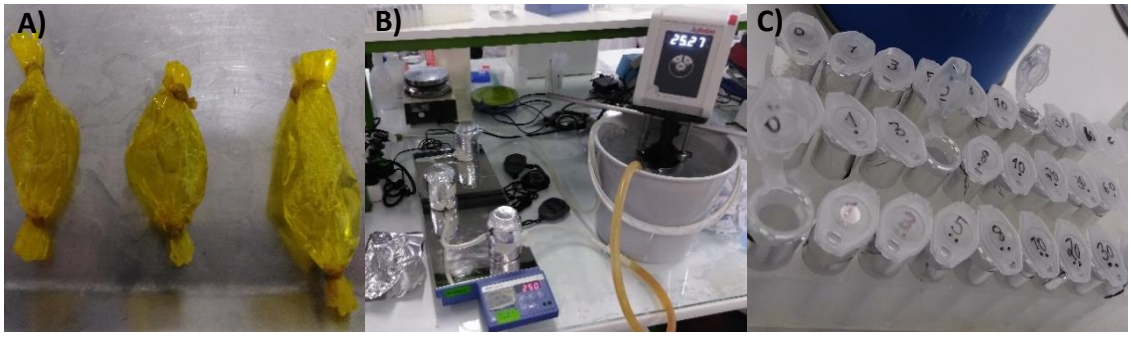

Figure 4. Representative image of A) dialysis membranes, B) experimental mechanism, and C) collection of samples used in release kinetics assays

3.6.2. Mathematical modelling

Curcumin' release profile was evaluated using the linear superimposition model (LSM), a kinetic model which enables a mathematical simulation accounting for both Fickian and Case II transport effects in hydrophilic matrices (Pinheiro et al., 2015; Berens et al.,1979; Rivera et al., 2015)

$$M_t = M_{t,F} + M_{t,R} \qquad \text{Eq 3}$$

where, M_t represents the total mass of compound released from the protein nanostructure, being $M_{t,F}$ and $M_{t,R}$, the contributions of the Fickian and relaxation processes, respectively, at time t.

The Fickian diffusion process can be described as the 'uniform sphere model' through the following equation (Berens et al., 1978):

$$M_{t,F} = M_{\infty,F}\left[1 - \frac{6}{\pi^2}\sum_{n=1}^{\infty}\frac{1}{n^2}\exp\left(-n^2 k_F t\right)\right] \qquad \text{Eq 4}$$

where $M_{\infty,F}$ is the equilibrium amount of sorption released by Fickian diffusion in the unrelaxed polymer matrix and the k_F represents the Fickian diffusion rate constant. This model assumes that the Fickian contribution is driven by a gradient related to the invariant equilibrium concentration. The relaxation terms in equation 5 (bellow) are independent of particle size and are related to the dissipation of swelling stresses induced by entry of the penetrant (Berens et al., 1978).

$$M_{t,R} = \sum_i M_{\infty,R_i}\left[1 - \exp\left(k_{R_i} t\right)\right] \qquad \text{Eq 5}$$

where, M_{∞,R_i} are the contributions of the relaxation processes for compound release and k_{R_i} is the relaxation rate constant at the i^{th} polymer relaxation. Usually, there is only one main polymer relaxation that influences transport and thus the above equation can be simplified using $i = 1$.

Finally, the linear superimposition model can be simplified and described by the following equation:

$$\frac{M_t}{M_\infty} = X\left[1 - \frac{6}{\pi^2}\exp\left(-k_F t\right)\right] + (1-X)[1-\exp\left(k_R t\right)] \qquad \text{Eq 6}$$

Where, X is related to the fraction of compound released by Fickian transport. Equation 6 was used as a function for the application of the linear superimposition model to the experimental results. This intends to simulate the transport mechanisms involved in curcumin release through LF nanohydrogels (Bourbon et al., 2016).

3.7. Incorporation of nanohydrogels into model food matrices

3.7.1. Preparation of gelatine incorporating nanohydrogels

Unflavoured neutral gelatine (ROYAL) was purchased at a local hypermarket in Braga, Portugal. Gelatine has the following nutritional information (per 100 g of the product): energy: 1505 kJ (355 kcal); lipids: <0.1 g, of which saturated: <0.1 g, carbohydrates: 0.5 g, of which sugars: 0.5 g; proteins: 88.0 g; and salt: 0.73 g. Gelatine solutions were prepared as described in packaging instructions, with some modifications. Briefly, 0.052 g of nanohydrogels (prepared as described in section 3.3.1) were added to 1 g of gelatine, followed by a gentle mixing of both powders. This mass of nanohydrogels was fixed after a scanning of different nanohydrogel-gelatine ratios. Therefore, by varying the mass of nanohydrogels, it was determined that 0.052 g was the ideal amount of nanohydrogels (maximum solubility) to be added to the gelatine powder which corresponds to the proportions of this gelatine' recipe. Then, 10 mL of distilled water at 20 °C were added to the powder mixture and, after a gentle stirring, 40 mL of distilled water at 45 °C were finally added to the gelatine solution. In order to obtain a homogeneously dispersed gelatine, the solutions were placed in a water bath (open-system) at 45 °C, under magnetic stirring at 250 rpm, during 8 min. Gelatine control solutions were prepared in the same way, as described above, but without the addition of the nanohydrogels. The final solutions were placed into regular flasks, protected from light and stored at 4 °C, until gelation process is complete.

3.7.2. Absorption measurements

Two distinct samples of gelatine (prepared as described in the previous section), with and without nanohydrogels, were spectrophotometrically characterized using an UV-Vis spectrophotometer (Jasco V-560, Japan). Gelatine samples, previously stored at 4 °C, were liquified at 30 °C in a water bath (open-system), in order to facilitate their use and analysis. Therefore, samples (diluted 3x) were placed into a quartz cuvette with a path length of 1.0 cm. The absorbance spectra were recorded in the wavelength range between 250 and 500 nm with 2.0 nm of resolution and a band width of 1.0 nm. For a proper acquisition of curcumin absorbance spectrum, samples were diluted in a ratio of 1:3 and measured in triplicate. At the spectra raw data, they were subtracted the respective backgrounds, eliminating potential noise signals, as well as the gelatine absorbance signal, since gelatine has a significant contribution at the near UV spectral zone.

3.7.3. Fluorescence measurements

In order to obtain a qualitative analysis of nanohydrogels incorporated in gelatine matrix, their fluorescence emission was accessed in a spectrofluorometer (Horiba Scientific, USA) equipped with a standard cell holder. All sample preparation procedures used in the previous section were replicated for these fluorescence measurements. Then, samples (diluted 3x) were placed into a quartz cuvette with a path length of 1.0 cm and fluorescence emission spectra were caught in the wavelength range between 330 and 650 nm, with a resolution of 1.17 nm, 1 accumulation and an integration time of 0.1 s. The excitation wavelengths were set at 280 nm and 425 nm for LF and curcumin, respectively. The resulting spectra were already presented with the subtractions of background and control spectra, in order to discount their contributions at the final emission fluorescence spectrum.

3.8. Statistical analysis

3.8.1. Analysis of experimental data

During this study, statistical analyses were performed to every data from each of the experimental results. Therefore, the mean values and standard deviations of the experimental data were calculated. Statistical analysis of the data was carried out using Analysis of Variance (ANOVA) and Tukey mean comparison test ($p < 0.05$), resorting Origin® Pro 8 software (Massachusetts, USA).

3.8.2. Non-linear regression analysis

Equation 6 was fitted to data by non-linear regression using STATISTICA 10.0 software (Statsoft. Inc, USA). The Levenberg–Marquardt algorithm was applied towards the least squares function minimization. The quality of the regressions was evaluated based on the determination of correlation coefficient, R^2, the root mean square error (RMSE) and residuals visual inspection for randomness and normality. R^2 and sum of squared errors (SSE) were obtained directly from the software. The precision of the estimated parameters was evaluated by the standardised halved width (SHW %), which was defined as the ratio between the 95 % standard error (obtained from the software) and the estimate value (Pinheiro et al., 2015)

CHAPTER 4 – RESULTS AND DISCUSSION

4.1. Lactoferrin-curcumin association efficiency

Lactoferrin (LF) nanohydrogel system showed to be able to associate curcumin with an efficiency of 90 ± 1.09 % and loading capacity (LC) of 2.6 ± 0.02 %, for curcumin at 80 μg/mL (as shown in Figure 5). Above this concentration, the system can also associate curcumin, but it showed to be unstable since forms a curcumin precipitate after 3 days of storage at refrigerated conditions (i.e., 4 °C). This may be explained by the fact that the loading capacity of LF nanohydrogels was exceeded for curcumin concentrations above 80 μg/mL. Regarding the LC, it is possible to observe an evident increasing LC in function of curcumin concentration (Figure 5. B)). This clearly shows that LF nanohydrogels are able to load curcumin with a maximum concentration of 80 μg/mL. These results are in agreement with those obtained for AE, thus allowing us to select the 80 μg/mL as the optimal curcumin concentration for the following characterization and application methodologies. As a matter of fact, curcumin has a water solubility of approximately 3.12 μg/mL. However, curcumin is ca. 23 times more soluble when incorporated into these nanosystems than freely dispersed in water. This increased value was found out by dividing curcumin concentration in LF solution (72 μg/mL) (resulting value after multiplying 80 μg/mL by its AE value) by curcumin maximum concentration in water (maximum solubility). It is also notable that curcumin presented higher solubility within the LF nanohydrogels rather than other related aqueous systems related in scientific research (Teng et al., 2012; Aditya et al., 2015). Teng et al., (2012) reported the development of curcumin-loaded soy protein isolate nanoparticles with curcumin solubility around 30 μg/mL. Additionally, a study carried out by Aditya et al., 2015, related to β-Lactoglobulin-curcumin nanosuspensions, reported a maximum curcumin solubility of ca. 31 μg/mL.

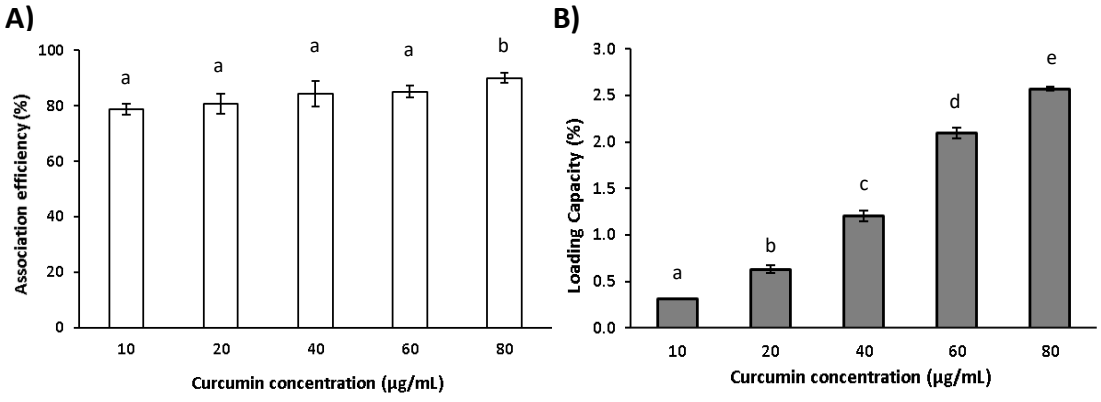

Figure 5. Effect of curcumin concentration on association efficiency A) and loading capacity B) of LF nanohydrogels. Data are presented as mean ± 95 % confidence interval. Different letters indicate statistically significant differences between values ($p < 0.05$).

4.2. Effect of heating time on nanohydrogels formation

4.2.1. Hydrodynamic diameter, polydispersity index and ζ-potential

As described by Bengoechea et al. (2011) the ideal temperature and holding time to promote LF denaturation and aggregation for the nanoparticle's formation are around 75 °C and 20 min, respectively. According to Martins et al. (2016), at this temperature and holding time, it is possible to obtain LF nanoparticles with sizes around 100 nm and PdI values around 0.2. This may be explained by the fact that native LF presents two thermal transitions: the first around 60.4 °C (apo-lactoferrin form) and the second around 89.1 °C (holo-lactoferrin form) (Bengoechea et al., 2011). In order to confirm the heating time period and obtain valuable indicators of such condition for nanohydrogels formation, the LF aqueous system was heated in a water bath (closed system) at 75 °C for 0, 5, 10, 15 and 20 min. Therefore, in this section the effect of increasing heating times from 0 to 20 min on size, PdI and ζ-potential of LF nanohydrogels at 75 °C will be evaluated. Figure 6 shows that nanoparticles exhibited a hydrodynamic diameter comprised between ca. 66 and 125 nm from 0 to 5 min of heating, remaining constant around 85 nm, from heating temperatures ≥ 10 min. This suggests that 10 min is the optimum heating time for nanohydrogels formation, thus meaning that a procedure optimization was possible with this study. At this temperature and holding time nanohydrogels exhibited size, PdI and a ζ-potential values of 84.9 ± 1.97 nm, 0.165 ± 0.012 and 23.4 ± 2.05 mV, respectively, thus corroborating the previous data found elsewhere (Martins et al., 2016). With the achievement of such results, less time and energy are necessary for the nanohydrogels preparation. The nanohydrogels ζ-potential values were between 21 and 25 mV during the DLS measurements, thus indicating that increasing heating times did not imply significant differences ($p > 0.05$) on the surface charge of LF nanoparticles and therefore, in the LF nanohydrogels formation. Regarding DLS analysis of curcumin incorporation, results (presented in Table 4) show a decrease in size and increase in PdI values as function of increasing curcumin concentration. These results may suggest that there is a shrink effect on nanoparticles shape until they reach the same size values of nanohydrogels without curcumin. On the opposite way, PdI values increased as function of curcumin concentration, which may be related with the potential formation of LF-curcumin aggregates. This occurrence may be explained by the fact that curcumin molecules tend to aggregate in aqueous solution, thus promoting

formation of clusters (Hazra et al., 2014). Concerning ζ-potential values, no statistically significant differences were observed after curcumin association (results not shown).

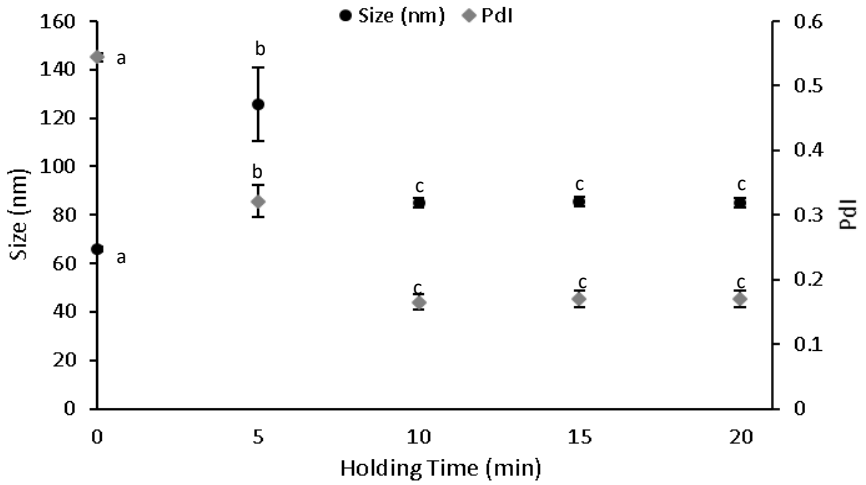

Figure 6. Effect of heating time on size and PdI of LF nanohydrogel, where data are presented as mean ± 95 % confidence interval. Different letters indicate statistically significant differences between values ($p < 0.05$).

Table 4. Effect of curcumin concentration on size and PdI of LF nanohydrogels, where data are presented as mean ±95% confidence interval. Different letters indicate statistically significant differences between values ($p < 0.05$).

µg/mL	**10**	**20**	**40**	**60**	**80**
Size (nm)	118.9±0.9^{a}	115.2±2.8^{a}	102.2±2.8^{b}	109.1±2.3^{c}	89.4±2.2^{d}
PdI	0.15±0.02^{a}	0.16±0.02^{b}	0.17±0.02^{c}	0.17±0.01^{c}	0.2±0.019^{c}

In addition, freeze dried nanohydrogels were also evaluated in terms of size and PdI, after dissolving both LF (control) and LF-curcumin powders in the aqueous media, described in sections 3.2.1 and 3.2.2, respectively. The resulting values for LF-curcumin solutions were 175.76 nm and 0.245 for size and PdI, respectively. Therefore, comparing the solutions before and after dehydration, the system has increased in size and maintained homogeneity, indicating the occurrence of aggregation and/or the formation of curcumin clusters in this process, as it was suggested above. Regarding LF solution (control), size and PdI values were approximately 147.13 nm and 0.422, respectively. These results show that the freeze drying may have promoted protein aggregation. Moreover, PdI values from LF control solutions denote a substantial increase in solution heterogeneity, which may indicate denaturation of LF proteins, since they are no longer able to form a homogeneously dispersed nanohydrogel. On the opposite way, LF-curcumin solutions have responded differently to freeze drying process, showing acceptable size (comprised in the

nanometre scale) and PdI values (comprised between 0.1 and 0.3). Additionally, as it can be observed in Figure 7, LF and LF-curcumin powders present different forms which lead to the conclusion that molecules have packed in distinct ways.

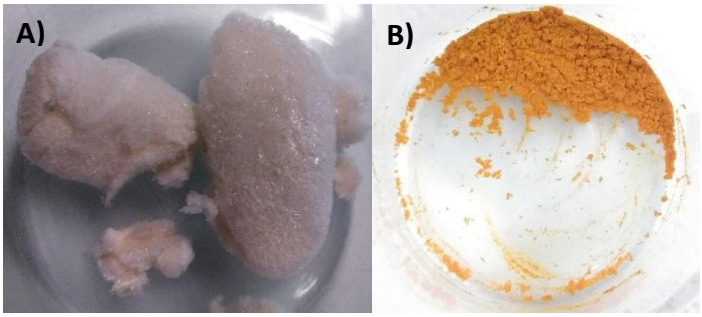

Figure 7. Representative images nanohydrogels after lyophilization: A) LF and B) LF-curcumin.

4.2.2. Turbidity

Temperature and holding time are two of the most important parameters that affect LF nanohydrogels formation, since it promotes conformational changes in protein structure, and therefore in LF aggregation. The turbidity was measured to monitor the effect of increasing heating time on LF aggregation. As it can be observed in Figure 8, the turbidity of LF nanohydrogels increased as function of heating time. Initially, at 0 min of heating (right before thermal treatment), there is no evidence of protein aggregation, since LF structures are dispersed in the aqueous solution. This behaviour can be visualized by naked eye (as shown in Figure 9), where it is easily observed the increase in turbidity of LF solutions as function of increasing heating time. Although turbidity is still raising from 10 to 20 min, there are no visual differences on the respective samples (i.e., 10, 15 and 20 min). However, increasing turbidity values indicate an increase on protein aggregation. These results are in agreement with previous research work (Martins et al., 2016).

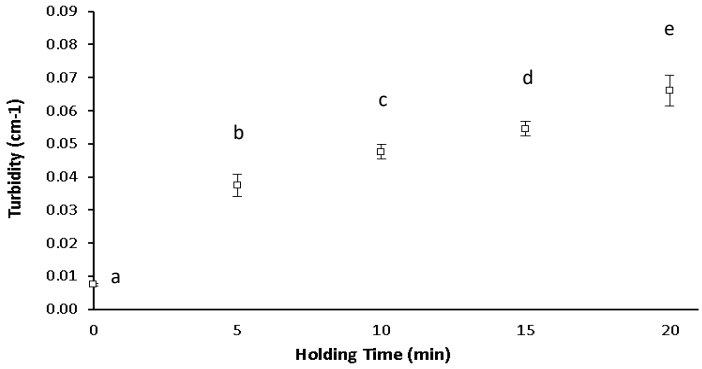

Figure 8. Effect of heating time on LF nanohydrogels turbidity, where data are presented as mean ± 95 % confidence interval. Different letters indicate statistically significant differences between values ($p < 0.05$).

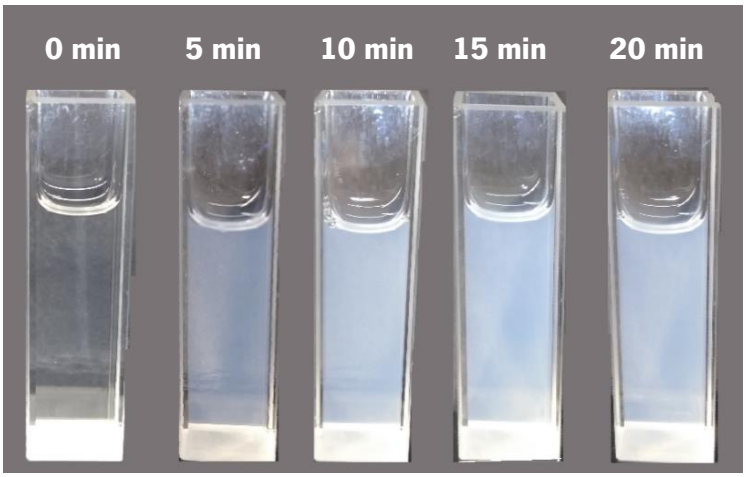

Figure 9. Representative image of LF aqueous solutions turbidity as function of thermal treatment at 75 °C for increasing heating time (from 0 to and 20 min).

4.2.3. Determination of nanohydrogels intrinsic fluorescence

The intrinsic fluorescence analysis was performed in order to evaluate the effect of increasing heating time on LF fluorescence emission. Tryptophan (Trp) is the main fluorophore responsible for proteins fluorescence emission and it is highly sensitive to its surrounding environment. Therefore, Trp residues can be used to monitor conformational changes in proteins (St et al. 2012). Red and blue shifted emission peaks correspond to the residue's exposure to a polar and a non-polar environment, respectively.

As it can be visualized in Figure 10, along with increasing heating time, the fluorescence emission peaks red shifted from 334 nm to 337 nm. Additionally, the fluorescence intensity is increasing from 0 to 20 min, reaching its maximum at 10 min of heating time, which statistically differs from the initial intensity at 0 min. This occurrence indicates that LF proteins are starting to unfold, thus allowing Trp residues (responsible for proteins fluorescence emission) initially located in proteins core to be exposed to a more polar environment. Lakowicz, (2006) refered to proteins emission maxima as a reflection of the average exposure of Trp residues to the aqueous phase. This consideration together with the results reported below suggest that at 10 min of heating time, the hydrophobic residues of LF are highly exposed and available to bind, thus favouring potential interactions with lipophilic compounds. As the purpose of this experiment is to validate and optimize the development of LF nanohydrogels aiming at reducing time and energy consumption, these results corroborate with previous ones. Being so, 10 min were fixed as the ideal heating time for the thermal treatment.

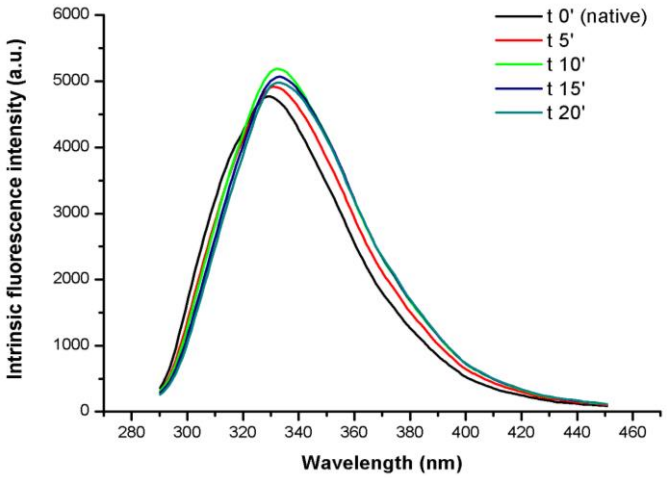

Figure 10. Effect of heating time on intrinsic fluorescence emission spectrum of LF nanohydrogels.

4.2.4. Determination of nanohydrogels extrinsic fluorescence

As a strategy to monitor variations on the accessibility of LF hydrophobic areas, an extrinsic fluorescence measurement was performed. LF solutions were heated at 75 °C from 0 to 20 min and, further on, a LF-ANS complex was formed. This thermal treatment may have caused conformational changes in protein structure and as such, ANS fluorescence emission spectra were recorded for each condition. ANS probe is considered an extrinsic fluorophore that exhibits its fluorescence emission when bind to proteins hydrophobic sites. For instance, the quantum yield of ANS is about 0.002 in aqueous medium, but near 0.4 when bound to serum albumin (Lakowicz, 2006). As it can be visualized in Figure 11, ANS fluorescence emission increased as function of increasing heating time, thus suggesting that more hydrophobic sites become available. From 10 to 20 min there are no statistically significant differences ($p < 0.05$). These results are in agreement with previous research studies related to LF extrinsic fluorescence (Li et al., 2018; Stănciuc et al., 2013).

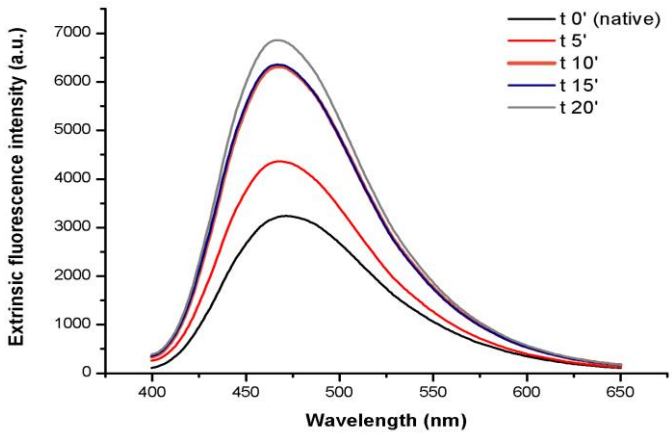

Figure 11. Effect of heating time on extrinsic fluorescence emission spectrum of LF nanohydrogels.

4.3. Evaluation of protein-ligand interaction

4.3.1. Evaluation of curcumin-ANS competition for LF hydrophobic sites

To evaluate the potential hydrophobic interactions between LF and curcumin, an ANS probe extrinsic fluorescence measurement was carried out for a range of curcumin concentrations between 10 and 80 µg/mL. Since curcumin presents a lipophilic character, it is expected that this compound may associate with LF hydrophobic residues rather than any other sites. As it can be observed in Figure 12, at lower curcumin concentration (i.e., 10 µg/mL) ANS still fluoresced, while for higher concentrations (i.e., 20, 40 and 80 µg/mL), the fluorescence intensity signal of ANS presented an abrupt loss, thus suggesting that curcumin is occupying the majority of LF hydrophobic sites. Therefore, these results revealed a curcumin-ANS competition for LF hydrophobic sites. It is notable that as the concentration of curcumin increased, the fluorescence intensity maxima of ANS red shifted, where at the minimum concentration of curcumin, the ANS peak was already red shifted comparing to a control, as observed in the previous section. Therefore, since ANS was added to the nanohydrogel solutions after curcumin association, these shift events may have occurred through two possible ways, or just both together. These are: the contribution of curcumin fluorescence intensity maximum, since curcumin is also excited at 370 nm (besides the subtraction of curcumin fluorescence emission data) and/or ANS molecules may have been linked through electrostatic interactions (Stănciuc et al., 2013). These kinds of interaction are less strong than the hydrophobic ones, resulting in an energetically unfavourable binding process. Proteins and phenols interaction mechanisms have been reported to be recognized as hydrogen bonding, hydrophobic interaction, and pi–pi stacking (Siebert et al., 1996; Teng et al., 2014).

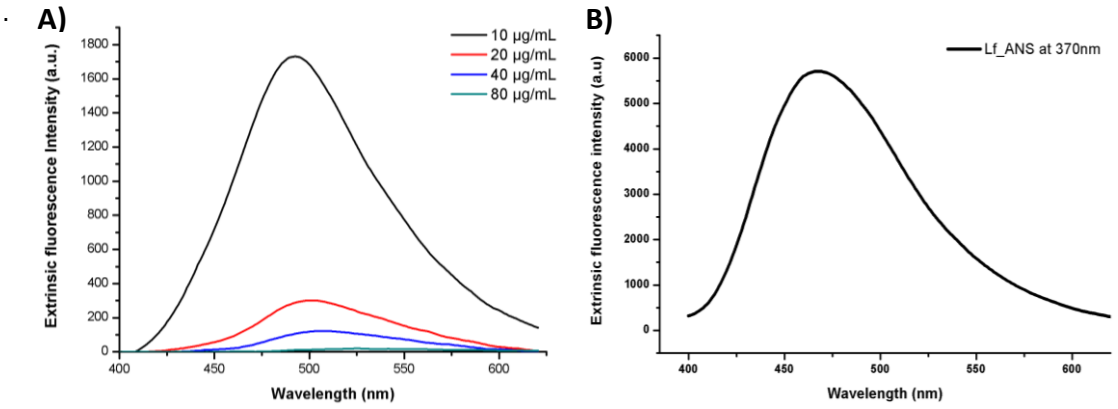

Figure 12. Extrinsic fluorescence spectra representing: the effect of increasing curcumin concentration on ANS emission A) and on ANS emission without curcumin (control) B).

4.3.2. Evaluation of LF secondary structure

In proteins secondary structure, α-helix configuration is usually characterized either by a positive band at 190 nm, and two negative peaks at 208 and 220 nm (Furtado et al. 2018). In the case of a β-sheet configuration, it presents a negative dichroic peak at 215 nm, which can be visualized in Figure 13. A) from 0 min of heating time to even 15 min. Native Lf form presented an ellipticity minimum near 210 nm (as shown in Figure 13. A)), where it shifted to high energy levels as function of heating time increased. These results suggest that LF nanohydrogels may adopt both α-helix and β-sheet configurations. The loss of CD signal magnitude (at 190 nm and between 210 and 235 nm) occurred progressively from 0 min (LF in native form) to 20 min of heating time, which may indicate that both configurations become more covered as a result of protein aggregation, during thermal treatment. These findings corroborate with previous ones described in sections 4.2.1 and 4.2.2, regarding nanohydrogels size and PdI, and turbidity, respectively. Concerning curcumin incorporation, the CD spectra shown differences between LF nanohydrogels and LF-curcumin nanohydrogels for the positive band recorded at 190 nm, which can be related to a slightly modification occurred in α-helix configuration. Nevertheless, both configurations still evidenced in LF-curcumin CD spectrum, as well as in both controls. These results may indicate that curcumin association did not affect LF secondary structure at a significant level, thus suggesting that curcumin did not interact with LF through its secondary structure binding sites.

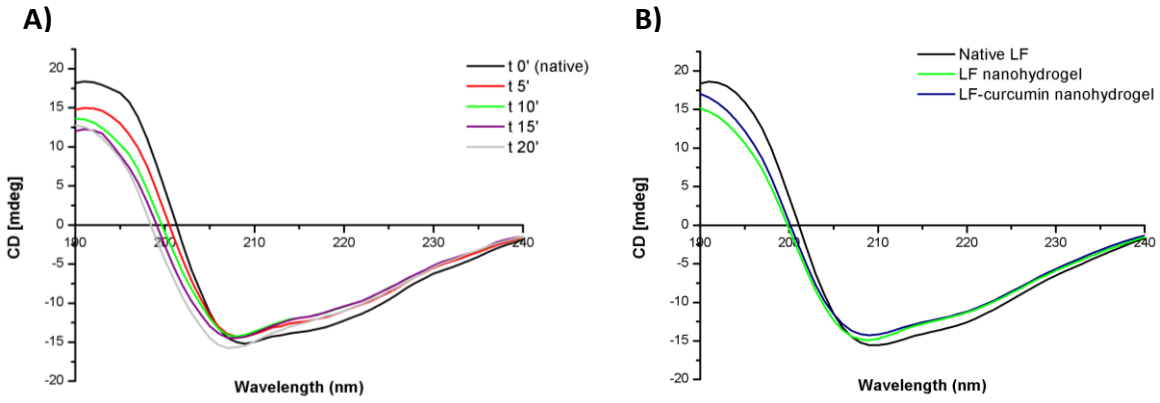

Figure 13. CD spectra showing the effect of A) increasing heating time (i.e., 0, 5, 10, 15 and 20 min) on LF secondary structure and of B) curcumin association to LF nanohydrogels.

Figure 14 represents the CD spectra recorded from LF and LF-curcumin samples after freeze-drying process. Both spectra were overlapped by LF and LF-curcumin nanohydrogels previously represented in Figure 13. B) with the purpose to evaluate the possible differences in between.

Regarding freeze-dried LF-curcumin and LF spectra, there is an increase in signal magnitude near 190 nm for both, evidencing the α-helix configuration. Furthermore, at 208 nm there is an evident increase on signal magnitude of freeze-dried LF, which suggests that the α-helix configuration of LF secondary structure may be more uncovered after lyophilization.

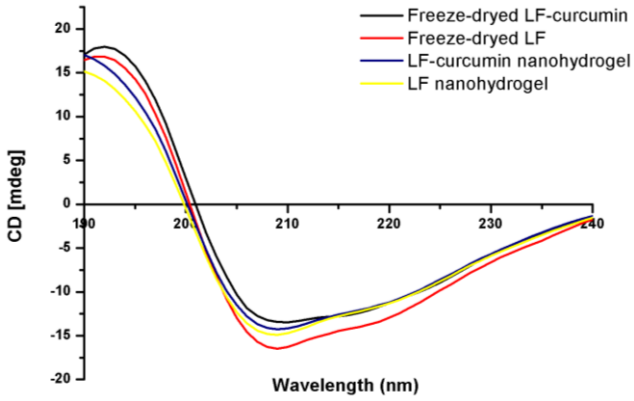

Figure 14. CD spectra showing the effect of freeze-drying process on LF and LF-curcumin nanohydrogels.

4.3.3. Analysis of LF-curcumin IR spectrum

FTIR measurements were performed to evaluate possible interactions between LF nanohydrogels and curcumin after its association. Figure 15 shows the combined spectra of LF nanohydrogels, LF-curcumin nanohydrogels and curcumin, respectively. LF nanohydrogels with and without curcumin were previously freeze-dried as described in section 3.3.1 and further analysed. Curcumin was used in its pure form in order to obtain an accurate IR signal. From the IR spectra, it is observed a curcumin characteristic stretching band (OH) and intra-molecular H bond at 3508 cm^{-1}, which is also characteristic of phenol group. Another characteristic peak of curcumin can be visualized at 1504 cm^{-1}, which corresponds to the C=O stretching, CCC and CC=O in plane bending (Mohan et al., 2012). It is also possible to observe a shift from 1504 cm^{-1} in pure curcumin to 1516 cm^{-1} (blue ellipses) in LF-curcumin nanohydrogels, suggesting that an interaction may have occurred between curcumin and nanohydrogel matrix. C=O stretching in plane bending of CCH is characterized by a peak at 962 cm^{-1}, which can also be observed in the IR spectra of pure curcumin (Mohan et al., 2012). After LF and curcumin mixture it is shown a shift to 971 cm^{-1} (red ellipses). The peak at 713 cm^{-1} of aromatic in plane bending (skeletal CCH and aromatic CCH, C=C stretching) of curcumin shifted to 773 cm^{-1} (black ellipses) after its association to nanohydrogels nets. These results are in the line with the behaviour observed for the association of curcumin and caffeine with LF-GMP nanohydrogels (Bourbon et al., 2016).

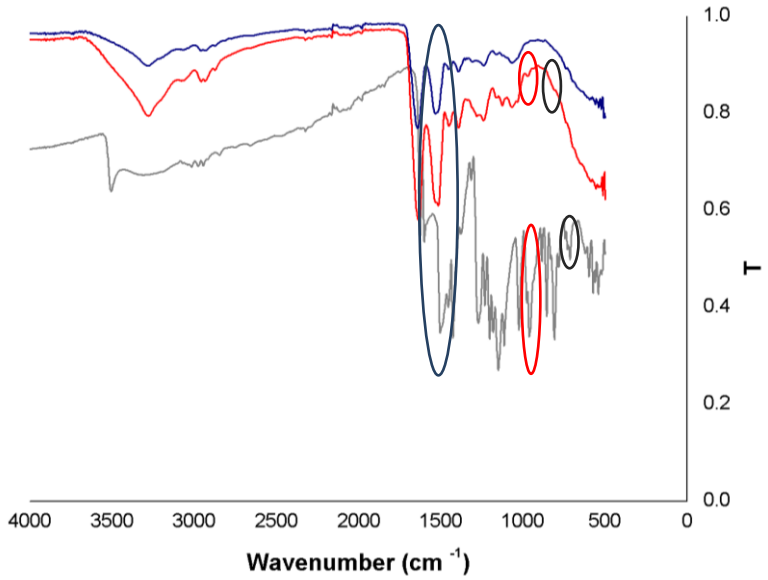

Figure 15. FTIR spectrum of LF nanohydrogels (–), LF-curcumin nanohydrogels (–) and curcumin (–) in the spectral region between 500 and 4000 cm^{-1}.

4.3.4. Evaluation of LF and curcumin fluorescence inhibition

Quenching refers to the decrease of fluorescence intensity of a compound and it can occur by a variety of processes such as collisional quenching, ground state complex formation, excited-state reactions, molecular rearrangements and energy transfer (Lakowicz, 2006). Within LF-curcumin interaction, it is observed a gradual decrease in fluorescence intensity of LF along with increasing concentrations of curcumin (Figure 16. A)). This may indicate that a quenching event occurred in this system, in which curcumin is the quencher candidate as it is added to LF nanohydrogel, thus resulting in a gradual decrease on LF fluorescence emission intensity. Additionally, it can be visualized a blue-shift in LF fluorescence spectra as the concentration increased, indicating that tryptophan and tyrosine residues started moving to a non-polar environment. This suggests that LF hydrophobic residues become buried or hidden due to curcumin association through hydrophobic interactions, which corroborates with previous analysis. Nevertheless, the fluorescence emission of curcumin also suffered an inhibition (as presented in Figure 16. B), which can be explained by the following hypotheses: i) since curcumin is associated to nanohydrogels, LF can act as a quencher in the case of binding to the aromatic rings of this compound, which are the main responsible for its fluorescence emission (Sneharani et al., 2010); ii) curcumin molecules are aggregating and consequently clusters are formed, which is somehow an expected behaviour for curcumin in aqueous solutions (Hazra et al., 2014); and iii) attenuation of the incident light by the fluorophore itself or other absorbing species. In addition, curcumin shifted to longer wavelengths

(Figure 16. B)) as function of increasing concentrations and such feature may be explained by the establishment of hydrogen bonds between curcumin and the solvent and/or LF and due to potential formation of curcumin aggregates (Lakowicz, 2006; Hazra et al., 2014).

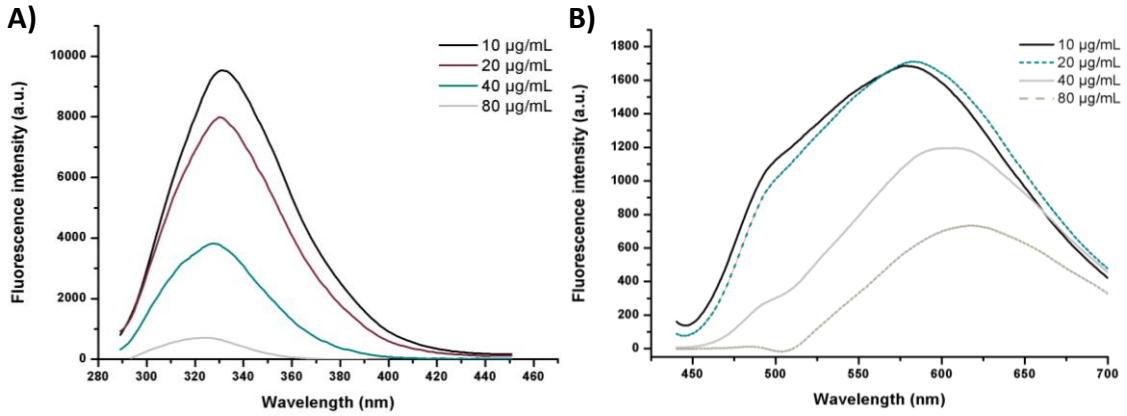

Figure 16. Effect of curcumin concentration on fluorescence emission spectra of LF-curcumin nanohydrogels when A) excited at 280 nm (tryptophan and tyrosine excitation wavelength) B) and excited at 425 nm (curcumin excitation wavelength).

4.3.5. Binding distance between LF and curcumin

FRET analysis is a powerful approach to estimate physical parameters related to biomolecules in solution. The spectral overlap obtained between LF fluorescence and curcumin absorbance (as shown in Figure 17) have shown that LF tryptophan and tyrosine residues (donor fluorophores in the excited state) may transfer non-radiative energy to curcumin chromophores (acceptor ligands in the ground state). This information is a good start point to confirm the occurrence of FRET phenomenon, which can provide accurate structural information important to determine protein-ligand binding distances (Diarrassouba et al., 2013).

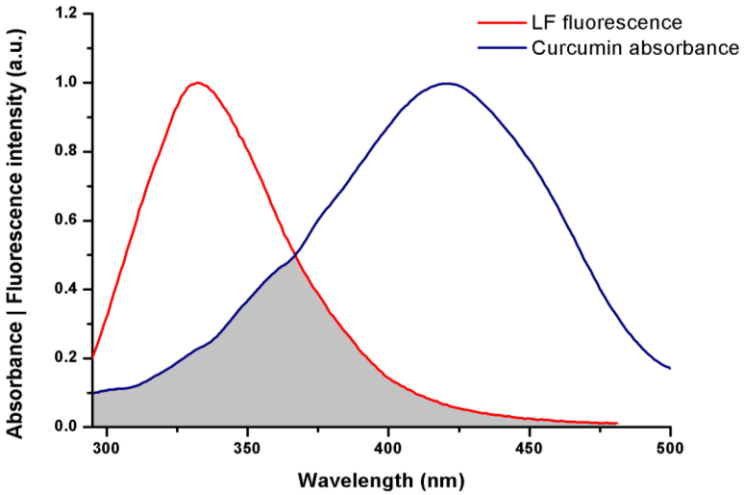

Figure 17. Representation of spectral overlap between LF fluorescence and curcumin absorbance.

FRET efficiency allows the determination of the binding distance r between the donor and acceptor. Therefore, calculations were made resorting to the following equations:

$$E = 1 - \frac{F}{F_0} \quad \text{Eq 6}$$

$$E = \frac{R_0^6}{R_0^6 + r^6} \quad \text{Eq 7}$$

where E is the efficiency of energy transfer between the donor and the acceptor, R_0 is the Förster distance (in Å), which represents the distance at which resonance energy transfer is 50 % efficient, and r is the distance between the donor (LF) and the acceptor (curcumin). F and F_0 correspond to the fluorescence intensities of LF with and without curcumin, respectively. R_0 can be calculated as follows in equation 8 (Diarrassouba et al., 2013).

$$R_0 = 9.78 \times 10^3 (K^2 n^{-4} \text{ø } J)^{\frac{1}{6}} \quad \text{Eq 8}$$

where, K^2 describes the relative orientation in space of the transition dipoles of the donor and acceptor, n is the refractive index of the solution, ϕ is the fluorescence quantum yield of the donor (LF), and the overlap integral J represents the degree of spectral overlap between the donor emission and the acceptor absorbance (Lakowicz, 2006).

$$J(\lambda) = \frac{\int_0^\infty F(\lambda)\varepsilon(\lambda)\lambda^4 \, d\lambda}{\int_0^\infty F(\lambda) \, d\lambda} \quad \text{Eq 9}$$

where $F(\lambda)$ is the corrected fluorescence intensity of the donor (LF) in the wavelength range from λ, $\varepsilon(\lambda)$ is the molar absorption coefficient of the acceptor (curcumin) at wavelength λ, n = 1.36, since the refractive index of biomolecules in solution ranges between 1.3 and 1.4, and ϕ = 0.118 (Horrocks et al., 1981).

There is an important criterium related to distance r and FRET phenomena, which needs to be clarified. Lakowicz, (2006) reported that measurements of the distance r, are only reliable when r is ranging between $0.5R_0$ and $2R_0$. This may be explained by the fact that E is strongly dependent on distance, as it can be noticeable when analysing equation 7.

Under these experimental conditions, the distance corresponding to 50 % energy transfer from LF (4.34×10^{-6} mol/L) to curcumin (3.75×10^{-5} mol/L) can be estimated and all related data are shown in Table 5.

Table 5. Representation of energy efficiency transfer (E), Förster radius estimation (R_0), the distance (r) between the donor (LF) and the acceptor (curcumin) estimated values

E (%)	R_0 (nm)	r (nm)
50	1.99	1.99
56	1.99	1.91
80	1.99	1.58
20	1.99	2.51

The highlighted data in Table 5 (blue rectangle) corresponds to the efficiency of energy transfer that occurred in this system with the experimental conditions above mentioned. Therefore, it led to the determination of R_0 and r values, which may be reliable since they fit the criteria ($0.5R_0 < r$ distance $< 2R_0$ and between 1.5 and 9 nm) (Lakowicz, 2006).

4.3.6. Characterization of LF-curcumin nanohydrogels morphology

Nanohydrogels were morphologically characterized and evaluated resorting to TEM imaging (as shown in Figure 18). TEM images confirmed the size between 50 and 90 nm (determined by DLS) and shown the spherical shape of LF nanohydrogels before (Figure 18. A)) and after (Figure 18. B)) their association with curcumin. As it can be observed in Figure 18. B), the appearance of those blurry spots may be explained by an increase in proteins denaturation, thus meaning that before curcumin incorporation (Figure 18. A)), nanohydrogels exhibited a higher homogeneity in comparison with the ones after it. This result is in agreement with PdI values, previously discussed in section 4.2.1. In addition, comparing both images, it is observed that nanohydrogels size did not significantly change ($p < 0.05$) – as it was already seen in DLS analysis.

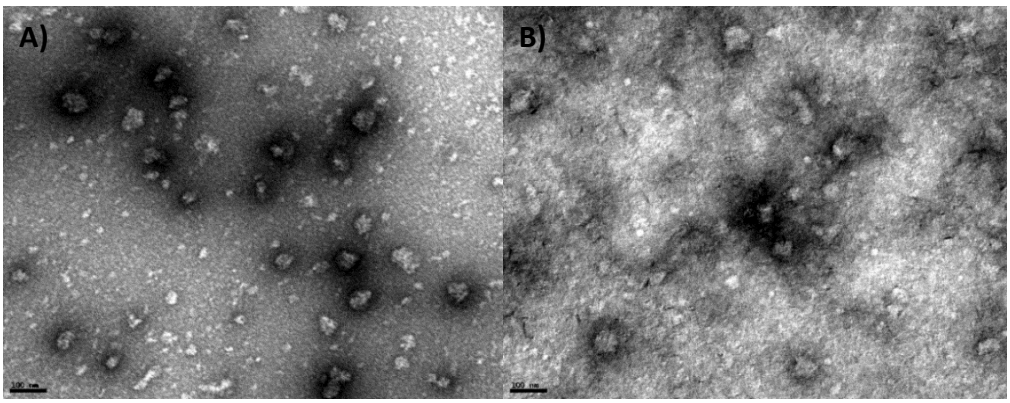

Figure 18. Transmission electron micrographs of A) LF nanohydrogels and B) LF-curcumin nanohydrogels (scale bar – 100 nm).

4.3.7. Native electrophoresis

This experiment was carried out with the purpose of understand what is happening with LF protein in terms of degradation, during the different processes at which LF was subjected. In Figure 19 it is possible to observe the characteristic mark of LF molecular weight (80 kDa) in all represented lanes (i.e., 1, 2, 3 and 4), which corroborates with previously reported values of LF weight (Stănciuc et al., 2013). Lane 1 corresponds to LF nanohydrogel and, besides the characteristic mark of LF molecular weight, there is a slightly tarnished zone between 100 and 150 kDa. This observation may be explained by LF aggregation at 10 min of heating time, resulting in bigger aggregates and consequently, higher molecular weight. As it can be visualized in lane 2, the process in which curcumin was incorporated in LF nanohydrogels may have caused a degradation or denaturation in LF proteins, in comparison with LF nanohydrogels (lane 1). These results are in agreement with TEM images, where the identified tarnish spots may have a relation with these blurry zones observed in electrophoresis lane 2. In addition, the lanes 3 and 4 that correspond to LF and LF-curcumin nanohydrogels after freeze-drying, respectively. Both lanes indicate that such process may implied some degradation and/or denaturation of LF proteins, as some blurry zones are more evidenced for lower molecular weight values.

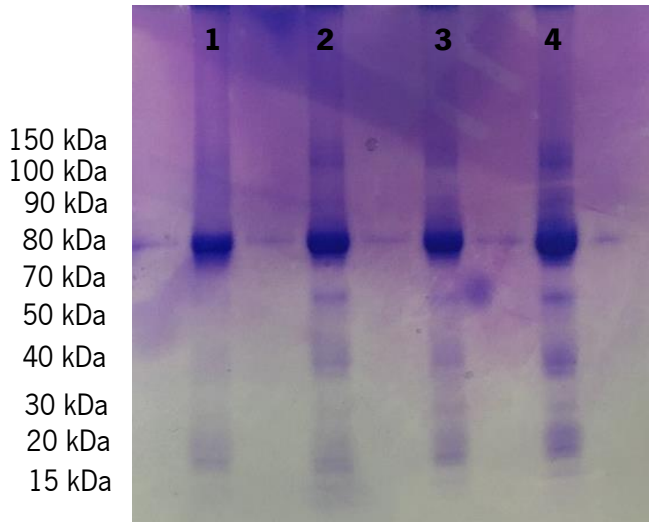

Figure 19. Native electrophoresis of LF (1) after nanohydrogels formation, (2) loaded with curcumin, (3) after nanohydrogels dehydration, and (4) after LF-curcumin nanohydrogels dehydration.

4.4. Nanohydrogels stability under storage conditions

4.4.1. Storage stability at 4 °C

During 35 days, LF-curcumin nanohydrogels shown constant stability at 4 °C, where solutions kept their orange-ish aspect, showing no signs of precipitate and possible contaminations. As it can be visualized in Figure 20, size and PdI values did not statistically differ ($p < 0.05$) for nanohydrogels with and without curcumin associated (results not shown). These results indicate that LF-curcumin nanohydrogels are well preserved under refrigerated storage conditions. In addition, ζ-potential values were always between ca. 16 and 21 mV.

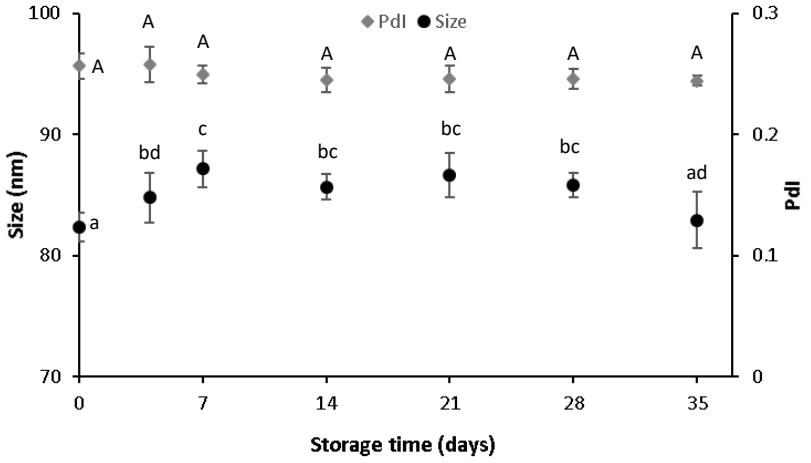

Figure 20. Effect of storage time at 4 °C on size and PdI of LF-curcumin nanohydrogels over 35 days, where data are presented as mean ± 95 % confidence interval. Different letters indicate statistically significant differences between values ($p < 0.05$), where higher-case and lower-case letters correspond to PdI and size values, respectively.

4.4.2. Storage stability at 25 °C

On the other hand, LF-curcumin nanohydrogels presented a loss in colour and the presence of curcumin precipitates at the bottom of each recipient, after 14 days for solutions stored at 25 °C. DLS measurements also shown significant changes ($p < 0.05$) in terms of size and PdI values, thus evidencing the nanohydrogels instability under room temperature conditions (Figure 21). Such variability in size and PdI values may indicate that there was an increase in denaturation degree of LF proteins, thus meaning that proteins can adopt different conformations and/or start to defragment, which may explain the appearance of curcumin precipitates at the bottom. These

results may be of valuable interest towards the selection of an appropriate food matrix for nanohydrogels incorporation.

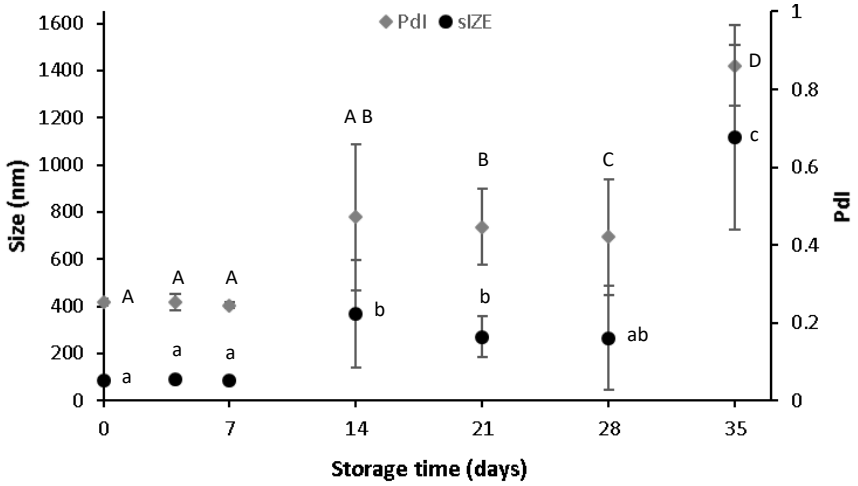

Figure 21. Effect of storage time at 25 °C on size and PdI of LF-curcumin nanohydrogels over 35 days, where data are presented as mean ± 95 % confidence interval. Different letters indicate statistically significant differences between values ($p < 0.05$).

4.5. Curcumin release kinetics in food simulants

4.5.1. Release profiles

The incorporation of micro- and nanostructures into food matrices towards the controlled release of nutraceuticals requires a proper understanding of the mechanisms involved in this process. Therefore, a release kinetics assay was performed in order to simulate curcumin release through LF nanohydrogels, into the food simulant media at 25 °C (harsh environmental conditions). The release rates of curcumin from LF nanohydrogels proved to be higher in the lipophilic food simulant rather than the hydrophilic one (Figure 22). It was also observed that, in the case of the hydrophilic food simulant, LF nanohydrogels net can retain curcumin more than 9 days, since only ca. 1.6 μg of curcumin was released during this period, reaching stabilization after ca. 4 h of release. At the second day of this experiment, it was noticed that there were no visual differences in the colour of the ethanol 10 % medium. This behaviour may be explained by the fact that this lipophilic compound presents a very low solubility in water ca. 0.0003 mg/mL at 25 °C (Bennet, 1992) . In the case of the lipophilic food simulant, ca. 16 μg of curcumin were released from LF nanohydrogels to the ethanol 50 % medium. The amount of curcumin released in this simulant was 10-fold higher comparing with the hydrophilic one. In addition, the release stabilization

occurred after ca. 7 h since the beginning of the experiment. In comparison, the release observed in both media, points out to a rapid stabilization occurring at the beginning of the experiment. This result may be explained by the possibility of curcumin being partially located on the surface of LF nanohydrogels (Bourbon et al., 2016). These findings suggest what should be the most appropriated food matrix character for this system, towards its application for functional foods. Moreover, as a measure to predict the physical mechanisms involved in curcumin release through protein matrix, a mathematical model was applied to the experimental values, after preliminary calculations.

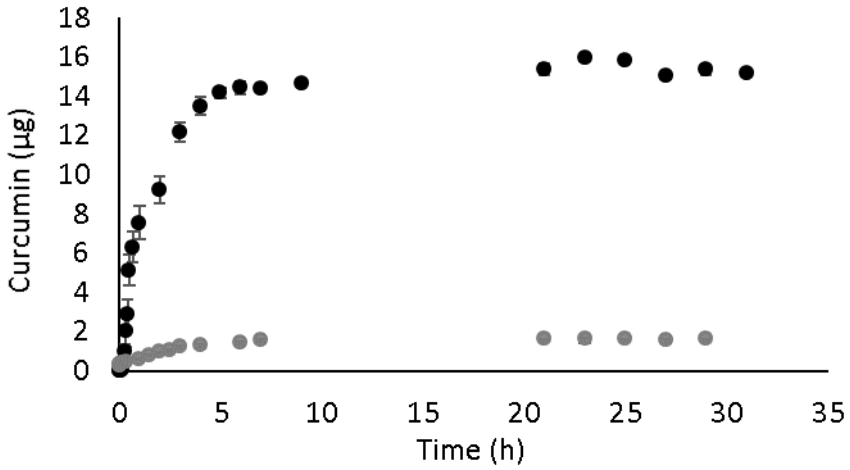

Figure 22. Release kinetics of curcumin from LF nanohydrogels into food simulant systems: (•) hydrophilic medium ethanol 10 % and (•) lipophilic medium ethanol 50 %.

4.5.2. Mathematical modelling

As it can be visualized below (Figure 23), a linear superimposition model (LSM) fitting progression was conducted in order to apply the most suitable mathematical modelling for curcumin release in both simulant media (ethanol 10 % and ethanol 50 %). Figure 23 shows the application of two different mathematical models, which intends to demonstrate the effect of Fick's diffusion model (Figure 23. A) and C)) and LSM model (Figure 23. B) and D)). The resulted graphs are a combination between the observed and the predicted values. For both simulant media, the R^2 presented a good regression quality, indicating that LSM curves fit adequately to the experimental data. Table 6 shows that the release mechanism in the hydrophilic simulant (ethanol 10 %) is mainly driven by Case II transport (polymer relaxation), since $X < 0.5$. Both relaxation and diffusion rate constants presented similar values, meaning that curcumin release occurred at the same rate for both Fick's diffusion and polymer relaxation, in ethanol 10 % ($k_F \approx k_R$). The release of curcumin

in the lipophilic simulant (ethanol 50 %) suggested that the predominant mechanism is Case II transport, where $X < 0.5$ (Bourbon et al., 2016). On the opposite way, Fickian diffusion model curves did not fit adequately to the experimental data for both media, as it can be visualized in Figure 23. A) and C). Regarding diffusion and relaxation rate constants, at these conditions, the respective data observed in Table 6 indicate that curcumin release occurred more rapidly by Fick's diffusion ($k_F > k_R$). (Martins et al., 2016). This behaviour may strengthen the hypothesis related to curcumin hydrophobic interactions, which was already discussed at the fluorescence analyses in the previous sections. Additionally, LF-curcumin solutions taken at the end of both release kinetics assays, were analysed by DLS in order to assess their size and PdI values. At the release kinetics assay with ethanol 50 %, the samples presented sizes and PdI values above 500 nm and 0.5, respectively (results not shown). This can be explained by the entry of the simulant medium through the membrane containing LF-curcumin solution, which may have caused LF precipitation due to the high ethanol concentration. On the other hand, LF-curcumin samples taken from release kinetics assay with ethanol 10 % presented 89.53 nm and 0.303 for size and PdI values, respectively, showing good stability until the end of the experiment.

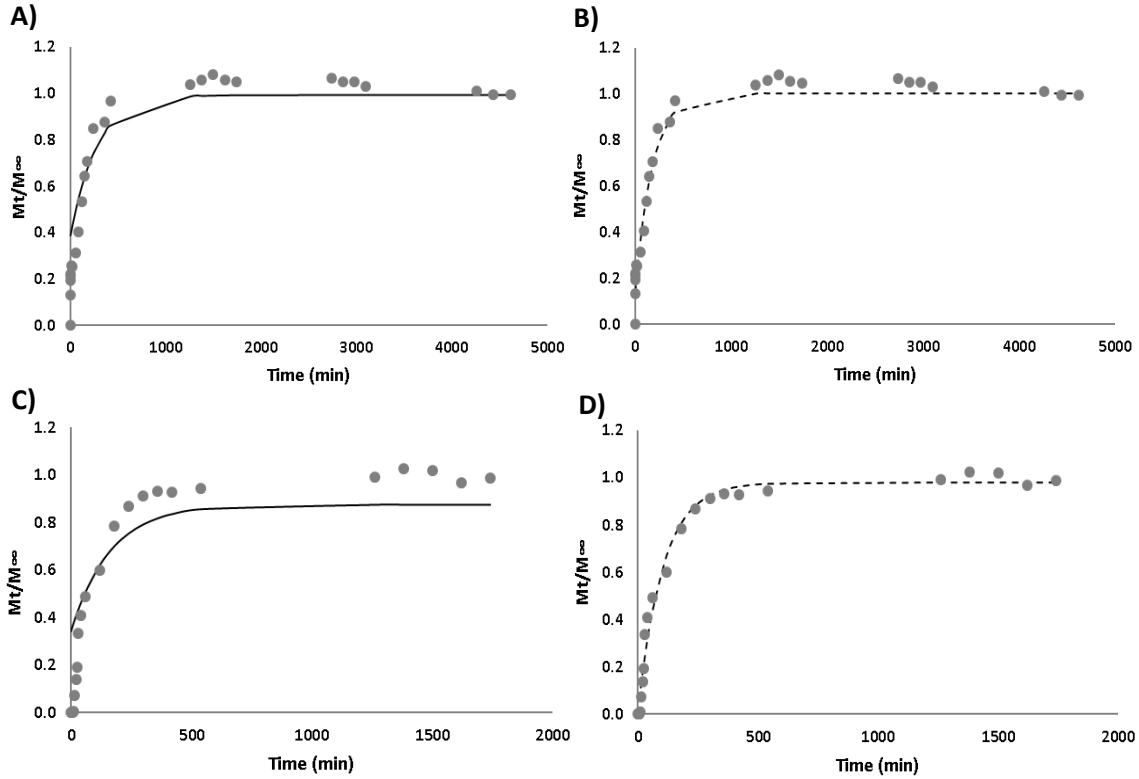

Figure 23. Experimental data representation of curcumin release (•) at hydrophilic medium ethanol 10 % (A) and B)) and lipophilic medium ethanol 50 % (C) and D)). Description of Fick's diffusion model (—) and linear superimposition model of curcumin release (- -) at 25 °C.

Table 6. Results of fitting the LSM (i=1) to experimental data of curcumin release profiles. Evaluation of the quality of the regression based on R^2 and *RMSE*.

Food simulant	T (°C)	R^2	RMSE	X	K_F (min^{-1})	K_R (min^{-1})
10 % ethanol	25	0.978	0.079	0.365	0.006	0.006
				(13.56 %)*	(15925.55 %)*	(5599.66 %)*
50 % ethanol	25	0.992	0.052	0.023	23.844	0.01
				(478.92 %)*	(0 %)*	(4.62 %)*

Note: RMSE - Root mean square error; X - The fraction of compound released by Fickian transport; K_F - Fickian diffusion rate constant and K_R - Relaxation *ith* rate constants. * Standardised halved width (*SHW %*).

4.6. Evaluation of nanohydrogels incorporation into a food matrix model

The nanohydrogels were incorporated into a gelatine matrix (used as a real food model) in order to evaluate the protein conformational changes when in contact with gelatine medium and to assess curcumin stability in such application. Figure 24 shown the visual aspect of gelatine incorporating LF-curcumin nanohydrogels (Figure 24. A)) and without nanohydrogels, as control (Figure 24. B)). After analysing these images, there are some considerations that should be highlighted, namely: i) the change in colour revealed that curcumin acted as colouring agent; ii) the incorporation of nanohydrogels did not affect gelatine transparency, and iii) the gelatine visual properties did not change after nanohydrogels incorporation. Gelatine samples were kept up to 7 days, and no visual changes were noticed at the end of this period.

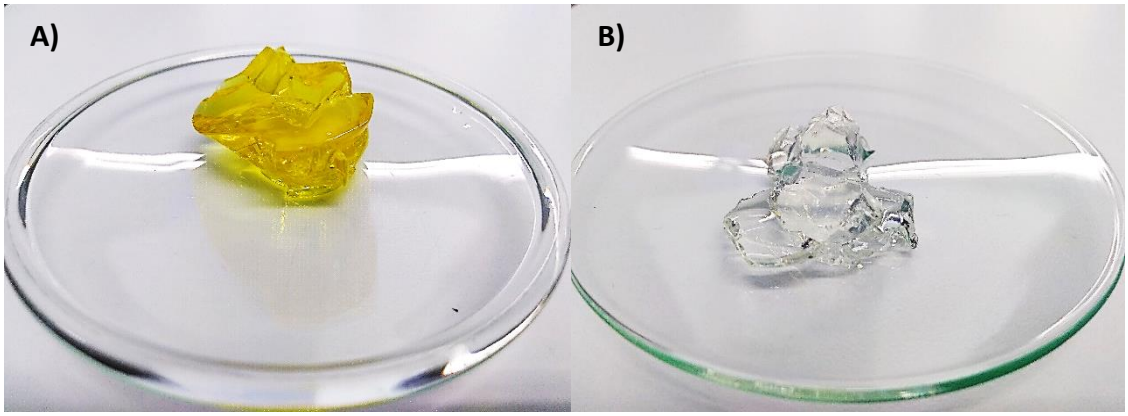

Figure 24. Representative images of gelatine A) containing and B) without nanohydrogels.

4.6.1. Absorption measurements

Absorbance spectra do not show sensitivity to molecular dynamics and can only provide information on the average solvent shell neighbouring the chromophore (Lakowicz, 2006). From Figure 25, it is possible to compare LF-curcumin nanohydrogels in the gelatine matrix and in the control (EtOH at 7.5 %, as described in section 3.2.2). Concerning the absorbance signal intensity, it has increased in aqueous solution (control) in comparison to the spectra obtained from LF-curcumin nanohydrogels in the gelatine matrix. This finding indicates that the chromophores presented in the control solution may have been more available to absorb light, rather the ones in gelatine. Since gelatine is a more complex matrix than water, LF and curcumin chromophores may have been hidden by such matrix, which appears to be a predictable behaviour. Collisional quenching occurrence only affects the excited states of the fluorophores, which can also be reflected in the absence of changes in absorbance spectra (as shown in Figure 25) (Lakowicz, 2006). This feature points out to the possibility of occurring such phenomena between the fluorophores and the surrounding solvent. However, to conclude whether quenching occurred, as well as to determine its type, further studies would be needed such as life-time fluorescence measurements with varying concentrations and excitation wavelengths for both LF and curcumin fluorophores.

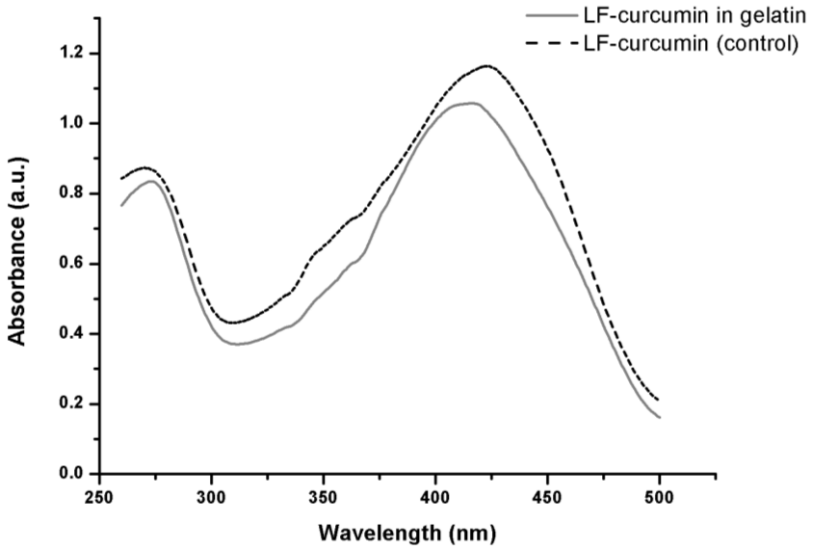

Figure 25. Effect of gelatine matrix on LF-curcumin nanohydrogels absorbance spectrum.

4.6.2. Fluorescence measurements

Fluorescence analysis can provide accurate information about protein conformational changes as a function of its behaviour when surrounded by environmental conditions with distinct polarities.

Additionally, different environments for the bound ligand may cause spectral shifts or change in quantum yield, which are usually reflected by binding phenomena. Regarding the fluorescence response of LF-curcumin nanohydrogels excited at 280 nm, there was a significant decrease in fluorescence intensity maximum, as well as an evident red-shift (Figure 26. A)). LF proteins presented an intensity maximum around 328 nm in aqueous solutions while it has shifted to 342 nm in gelatine matrix, which may indicate a rearrangement of tryptophan and tyrosine residues to a more polar environment (Lakowicz, 2006). It is also important to account that LF-curcumin nanohydrogels were incorporated into the gelatine matrix after freeze-drying process, and it may have provoked conformational changes on LF structure. It was also possible that gelatine have absorbed part of LF fluorescence emission, which may explain the low fluorescence intensity observed for LF. Comparing the emission spectra of LF-curcumin nanohydrogels (exciting curcumin at 425 nm) incorporated in gelatine matrix, in relation to the exhibited by the control in EtOH 7.5 % (Figure 26. B)), it was possible to visualize a red-shift of ca. 50 nm on fluorescence intensity maximum. Another interesting finding was that curcumin presented a higher emission intensity maximum in gelatine matrix when compared to the spectrum obtained from the aqueous solution (control). This deviation and intensity variations may be explained by curcumin solvatochromic nature, i.e., depending on the solvent polarity, shift and intensity variations are expected in curcumin spectra (Patra et al., 2011). Since curcumin is considered a lipophilic compound, it is expected to have lower affinity with polar solvents, which may be reflected by a decrease in its fluorescence signal. However, further studies are needed to evaluate and determine the interactions between LF-curcumin nanohydrogels and gelatine matrices.

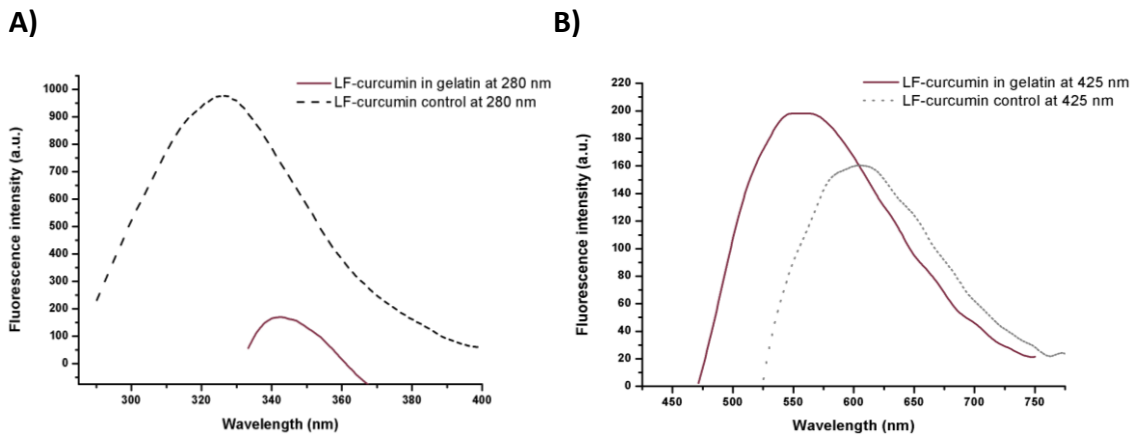

Figure 26. Effect of gelatine matrix on LF-curcumin nanohydrogel fluorescence spectra when compared to control for A) excitation at 280 nm, and B) excitation at 425 nm.

CHAPTER 5 – Conclusions and future work

5.1. Conclusions

LF nanohydrogels have the ability to associate lipophilic nutraceuticals, such as curcumin, with remarkable association efficiency and loading capacity values, thus making of such nanohydrogels a promising candidate to serve as vehicle for lipophilic nutraceuticals' controlled release.

Fluorescence measurements enabled the acquirement of valuable structural information about LF-curcumin interactions namely, that curcumin binds to LF mainly through hydrophobic interactions, which revealed to be a strong linkage. In this study, the analysis of FRET occurrence has contributed to infer LF-curcumin binding distances. In addition, it was also possible to verify that curcumin solubility, in aqueous solutions, was highly improved by its interaction with LF nanohydrogels, and that the resulting system (LF-curcumin nanohydrogels) was stable for 14 days (in stress conditions at 25 °C) but up to 35 days at refrigerated conditions (4°C). These findings allowed us to conclude that this system would be properly applied for longer periods of time in food products, where storage is processed under refrigerated conditions (4°C), rather than the ones processed at room temperature.

Curcumin release profiles suggested that hydrophilic food matrices are the most suitable ones for LF-curcumin nanohydrogels, since those are not able to trigger curcumin release from LF nanohydrogels to the food matrix medium. This finding is of great interest since it is expected that LF structure may hold curcumin after the incorporation in a gelatine until the moment of its digestion. Furthermore, curcumin release kinetics through LF nanohydrogels have shown to be mainly driven by Case II transport, rather than Fickian diffusion, in both simulants. These results have contributed to achieve fundamental knowledge in terms of both LF and curcumin behaviour in food simulants, which, in turn, may represent a valuable information towards its application into real food matrices.

Concerning the incorporation of this system into a model food matrix, gelatine proved to be, at a pilot scale, a suitable food model where the system remained soluble and stable up to 7 days. The spectroscopic techniques enabled a simple and rapid characterization as a qualitative method, since it was possible to assess both LF and curcumin absorbance and fluorescence spectra before and after their incorporation in gelatine matrix. Finally, the resulting spectra allowed to conclude that both LF and curcumin remained stable, without signs of degradation.

5.2. Future work and recommendations

As future work would be of great interest to evaluate the toxicity and the behaviour of LF-curcumin nanohydrogels through *in vitro* cytotoxicity and gastrointestinal model assays in order to assess if such nanosystems are safer for human consumption, stable and efficient for delivery of nutraceuticals. On that basis, it would be interesting to access the model nutraceutical bioaccessibility and bioavailability in order to validate nanosystems efficiency.

Moreover, an extensive characterization would be fundamental towards a better optimization of the incorporation of nanosystems into food matrices with different natures, characters and complexities. Thus, it would be needed to assess nutraceutical properties after its incorporation in food matrices, such as colorant parameters (in the case of a coloured nutraceutical), nutritional value and stability at different storage conditions over time.

Additionally, it would be necessary to evaluate the food matrices' properties before and after the incorporation of such nanosystems. This evaluation could be performed resorting to rheometry and texturometry in order to verify if some of the food matrix physical properties suffer modifications with the nanosystem addition. Finally, it would be fundamental to assess the food nutritional composition after the incorporation of a nanosystem into it.

Furthermore, an upgrade of the fluorometric study would be needed, towards a better understanding of protein-ligand interactions. To accomplish that, life-time fluorescence, synchronous fluorescence, quenching experiments and two photon absorption measurements may represent some of the available techniques for such characterization. In addition, it would be interesting to perform molecular dynamics and docking studies, as those may result in valuable fundamental knowledge in what protein structural information concerns.

References

Acevedo-Fani, A., Silva, H. D., Soliva-Fortuny, R., Martín-Belloso, O., & Vicente, A. A. (2017). Formation, stability and antioxidant activity of food-grade multilayer emulsions containing resveratrol. *Food Hydrocolloids*, 71, 207–215.

Aditya, N. P., Yang, H., Kim, S., & Ko, S. (2015). Fabrication of amorphous curcumin nanosuspensions using β-lactoglobulin to enhance solubility, stability, and bioavailability. *Colloids and Surfaces B: Biointerfaces*, 127, 114–121.

Al-Baarri, A. N., Hayashi, M., Ogawa, M., & Hayakawa, S. (2011). Effects of Mono- and Disaccharides on the Antimicrobial Activity of Bovine Lactoperoxidase System. *Journal of Food Protection*, 74(1), 134–139.

Akhavan Mahdavi, S., Jafari, S. M., Assadpoor, E., & Dehnad, D. (2016). Microencapsulation optimization of natural anthocyanins with maltodextrin, gum Arabic and gelatin. International *Journal of Biological Macromolecules*, 85, 379–385.

Arroyo-Maya, I. J., & McClements, D. J. (2015). Biopolymer nanoparticles as potential delivery systems for anthocyanins: Fabrication and properties. *Food Research International*, 69, 1–8.

Augustin, M. A., & Sanguansri, P. (2009). Chapter 5 Nanostructured Materials in the Food Industry. A*dvances in Food and Nutrition Research*, 183–213.

Azevedo, M. A., Bourbon, A. I., Vicente, A. A., & Cerqueira, M. A. (2014). Alginate/chitosan nanoparticles for encapsulation and controlled release of vitamin B2. *International Journal of Biological Macromolecules*, 71, 141–146.

Barbana, C., Pérez, M. D., Sánchez, L., Dalgalarrondo, M., Chobert, J. M., Haertlé, T., & Calvo, M. (2006). Interaction of bovine -lactalbumin with fatty acids as determined by partition equilibrium and fluorescence spectroscopy. *International Dairy Journal*, 16(1), 18–25.

Bennett, G. (1992). The merck index: An encyclopedia of chemicals, drugs and biologicals. *Journal of Hazardous Materials*, 30(3), 373.

Bengoechea, C., Peinado, I., & McClements, D. J. (2011). Formation of protein nanoparticles by controlled heat treatment of lactoferrin: Factors affecting particle characteristics. *Food Hydrocolloids*, 25(5), 1354–1360.

Berens, A., & Hopfenberg, H. . (1978). Diffusion and relaxation in glassy polymer powders: 2. Separation of diffusion and relaxation parameters. *Polymer*, 19(5), 489–496.

Berens, A. R., & Hopfenberg, H. B. (1979). Induction and measurement of glassy-state relaxations by vapor sorption techniques. *Journal of Polymer Science: Polymer Physics Edition*, 17(10), 1757–1770.

Betz, M., Steiner, B., Schantz, M., Oidtmann, J., Mäder, K., Richling, E., & Kulozik, U. (2012). Antioxidant capacity of bilberry extract microencapsulated in whey protein hydrogels. *Food Research International*, 47(1), 51–57.

Beztsinna, N., Solé, M., Taib, N., & Bestel, I. (2016). Bioengineered riboflavin in nanotechnology. *Biomaterials*, 80, 121–133.

Biesalski, H.-K., Dragsted, L. O., Elmadfa, I., Grossklaus, R., Müller, M., Schrenk, D., & Weber, P. (2009). Bioactive compounds: Definition and assessment of activity. *Nutrition*, 25(11-12), 1202–1205.

Blackshear, P. J. (1984). [12] Systems for polyacrylamide gel electrophoresis. *Part C: Enzyme Purification and Related Techniques*, 237–255.

Bourbon, A. I., Pinheiro, A. C., Carneiro-da-Cunha, M. G., Pereira, R. N., Cerqueira, M. A., & Vicente, A. A. (2015). Development and characterization of lactoferrin-GMP nanohydrogels: Evaluation of pH, ionic strength and temperature effect. *Food Hydrocolloids,* 48, 292–300

Brock, J. H. (2002). The physiology of lactoferrin. *Biochemistry and Cell Biology*, 80(1), 1–6.

Brownlow, S., Cabral, J. H. M., Cooper, R., Flower, D. R., Yewdall, S. J., Polikarpov, I., & Sawyer, L. (1997). Bovine β-lactoglobulin at 1.8 Å resolution — still an enigmatic lipocalin. *Structure*, 5(4), 481–495.

Burgain, J., Gaiani, C., Linder, M., & Scher, J. (2011). Encapsulation of probiotic living cells: From laboratory scale to industrial applications. *Journal of Food Engineering*, 104(4), 467–483.

Calo, J. R., Crandall, P. G., O'Bryan, C. A., & Ricke, S. C. (2015). Essential oils as antimicrobials in food systems – A review. *Food Control*, 54, 111–119.

Caruso, F., Hyeon, T., & Rotello, V. M. (2012). Nanomedicine. *Chemical Society Reviews*, 41(7), 2537.

Cerqueira, M. A., Pinheiro, A. C., Silva, H. D., Ramos, P. E., Azevedo, M. A., Flores-López, M. L., Rivera, M. C., Bourbon, A. I., Ramos, O. L., & Vicente, A. A. (2013). Design of Bio-nanosystems for Oral Delivery of Functional Compounds. *Food Engineering Reviews*, 6, 1–19.

Chen, G., Wang, H., Zhang, X., & Yang, S.-T. (2014). Nutraceuticals and Functional Foods in the Management of Hyperlipidemia. *Critical Reviews in Food Science and Nutrition*, 54(9), 1180–1201.

Chen, L., Remondetto, G. E., & Subirade, M. (2006). Food protein-based materials as nutraceutical delivery systems. *Trends in Food Science & Technology*, 17(5), 272–283.

Coates, J. (2000). "Interpretation of Infrared Spectra, A Practical Approach," *Encyclopedia of Analytical Chemistry* 10815–37.

Commission, E. (2011). Commission regulation (EU) on plastic materials and articles intended to come into contact with food. *In Official Journal of the European Union*, 1–89. No 10/2011 of 14 January.

Davidov-Pardo, G., Joye, I. J., & McClements, D. J. (2015). Food-Grade Protein-Based Nanoparticles and Microparticles for Bioactive Delivery. *Protein and Peptide Nanoparticles for Drug Delivery*, 293–325.

Desai, K. G. H., & Jin Park, H. (2005). Recent Developments in Microencapsulation of Food Ingredients. *Drying Technology*, 23(7), 1361–1394.

Desobry, S. A., Netto, F. M., & Labuza, T. P. (1997). Comparison of Spray-drying, Drum-drying and Freeze-drying for β-Carotene Encapsulation and Preservation. *Journal of Food Science*, 62(6), 1158–1162.

De Figueiredo Furtado, G., Pereira, R. N. C., Vicente, A. A., & Cunha, R. L. (2018). Cold gel-like emulsions of lactoferrin subjected to ohmic heating. *Food Research International*, 103, 371–379.

De Kruif, C. G., Weinbreck, F., & de Vries, R. (2004). Complex coacervation of proteins and anionic polysaccharides. *Current Opinion in Colloid & Interface Science*, 9(5), 340–349.

De Souza Simões, L., Madalena, D. A., Pinheiro, A. C., Teixeira, J. A., Vicente, A. A., & Ramos, O. L. (2017). Micro- and nano bio-based delivery systems for food applications: In vitro behavior. *Advances in Colloid and Interface Science*, 243, 23–45.

De Vos, P., Faas, M. M., Spasojevic, M., & Sikkema, J. (2010). Encapsulation for preservation of functionality and targeted delivery of bioactive food components. *International Dairy Journal*, 20(4), 292–302.

Diarrassouba, F., Liang, L., Remondetto, G., & Subirade, M. (2013). Nanocomplex formation between riboflavin and β-lactoglobulin: Spectroscopic investigation and biological characterization. *Food Research Internationa*l, 52(2), 557–567..

Dubey, B. N., & Windhab, E. J. (2013). Iron encapsulated microstructured emulsion-particle formation by prilling process and its release kinetics. *Journal of Food Engineering*, 115(2), 198–206.

Dunker, K. A. (2004). Current Topics Intrinsic Disorder and Protein Function". *Biochemistry.* 41 (21).

Ezhilarasi, P. N., Karthik, P., Chhanwal, N., & Anandharamakrishnan, C. (2012). Nanoencapsulation Techniques for Food Bioactive Components: A Review. *Food and Bioprocess Technology*, 6(3), 628–647.

Fagarasan, S., & Honjo, T. (2003). Intestinal IgA synthesis: regulation of front-line body defences. *Nature Reviews Immunology*, 3(1), 63–72.

Fahy, E., Subramaniam, S., Murphy, R. C., Nishijima, M., Raetz, C. R. H., Shimizu, T., Spener,F., van Meer, G., Wakelam, M. J. O., & Dennis, E. A. (2008). Update of the LIPID MAPS comprehensive classification system for lipids. *Journal of Lipid Research*, 50, S9–S14.

Floudas, C. A., Fung, H. K., McAllister, S. R., Mönnigmann, M., & Rajgaria, R. (2006). Advances in protein structure prediction and de novo protein design: A review. *Chemical Engineering Science*, 61(3), 966–988.

Gharsallaoui, A., Roudaut, G., Chambin, O., Voilley, A., & Saurel, R. (2007). Applications of spray-drying in microencapsulation of food ingredients: An overview. *Food Research International*, 40(9), 1107–1121.

Goers, J., Permyakov, S. E., Permyakov, E. A., Uversky, V. N., & Fink, A. L. (2002). Conformational Prerequisites for α-Lactalbumin Fibrillation. *Biochemistry*, 41(41), 12546–12551.

Gonçalves, C., Pereira, P., Schellenberg P., Coutinho, J., P., & Gama M., F. (2012). Self-Assembled Dextrin Nanogel as Curcumin Delivery System. *Journal of Biomaterials and Nanobiotechnology*, 2012, 3, 178-184.

Graveland-Bikker, J. F., Ipsen, R., Otte, J., & de Kruif, C. G. (2004). Influence of Calcium on the Self-Assembly of Partially Hydrolyzed α-Lactalbumin. *Langmuir*, 20(16), 6841–6846.

Greenfield, N. J. (2007). Using circular dichroism spectra to estimate protein secondary structure. *Nature Protocols*, 1(6), 2876–2890.

Gunasekaran, S., Xiao, L., & Ould Eleya, M. M. (2005). Whey protein concentrate hydrogels as bioactive carriers. *Journal of Applied Polymer Science*, 99(5), 2470–2476.

Gustafsson, L., Hallgren, O., Mossberg, A.-K., Pettersson, J., Fischer, W., Aronsson, A., & Svanborg, C. (2005). HAMLET Kills Tumor Cells by Apoptosis: Structure, Cellular Mechanisms, and Therapy. *The Journal of Nutrition*, 135(5), 1299–1303.

Gyarmati, B., Némethy, Á., & Szilágyi, A. (2013). Reversible disulphide formation in polymer networks: A versatile functional group from synthesis to applications. *European Polymer Journal*, 49(6), 1268–1286.

Hanker, J., & Giammara, B. (1987). Basic techniques for transmission electron microscopy. *Micron and Microscopica Acta*, 18(1), 41.

Hazra, M. K., Roy, S., & Bagchi, B. (2014). Hydrophobic hydration driven self-assembly of curcumin in water: Similarities to nucleation and growth under large metastability, and an analysis of water dynamics at heterogeneous surfaces. *The Journal of Chemical Physics*, 141(18), 18C501.

Hernández-Ledesma, B., Ramos, M., & Gómez-Ruiz, J. Á. (2011). Bioactive components of ovine and caprine cheese whey. *Small Ruminant Research*, 101(1-3), 196–204.

Horrocks, W. D., & Peter Snyder, A. (1981). Measurement of distance between fluorescent amino acid residues and metal ion binding sites. Quantitation of energy transfer between tryptophan and terbium(III) or europium(III) in thermolysin. *Biochemical and Biophysical Research Communications,* 100(1), 111–117.

Ipsen, R., & Otte, J. (2007). Self-assembly of partially hydrolysed α-lactalbumin. *Biotechnology Advances*, 25(6), 602–605..

Jain, A., Thakur, D., Ghoshal, G., Katare, O. P., & Shivhare, U. S. (2015). Microencapsulation by Complex Coacervation Using Whey Protein Isolates and Gum Acacia: An Approach to Preserve the Functionality and Controlled Release of β-Carotene. *Food and Bioprocess Technology*, 8(8), 1635–1644.

Kailasapathy, K., & Lam, S. H. (2005). Application of encapsulated enzymes to accelerate cheese ripening. *International Dairy Journal*, 15(6-9), 929–939.

Kang, Y., Yang, C., Ouyang, P., Yin, G., Huang, Z., Yao, Y., & Liao, X. (2009). The preparation of BSA-PLLA microparticles in a batch supercritical anti-solvent process. *Carbohydrate Polymers,* 77(2), 244–249.

Kehoe, J. J., & Brodkorb, A. (2014). Interactions between sodium oleate and α-lactalbumin: The effect of temperature and concentration on complex formation. *Food Hydrocolloids*, 34, 217–226.

Kelly, S. M., Jess, T. J., & Price, N. C. (2005). How to study proteins by circular dichroism. *Biochimica et Biophysica Acta (BBA) - Proteins and Proteomics*, 1751(2), 119–139.

Krasaekoopt, W., Bhandari, B., & Deeth, H. (2003). Evaluation of encapsulation techniques of probiotics for yoghurt. *International Dairy Journal*, 13(1), 3–13.

Kügler, M., Jänsch, L., Kruft, V., Schmitz, U. K., & Braun, H.-P. (1997). Analysis of the chloroplast protein complexes by blue-native polyacrylamide gel electrophoresis (BN-PAGE). *Photosynthesis Research*, 53(1), 35–44.

Kumar, V., Lemos, M., Sharma, M., & Shriram, V. (2013). Antioxidant and DNA damage protecting activities of Eulophia nuda Lindl. *Free Radicals and Antioxidants*, 3(2), 55–60.

Kwak, H. S. (2014). Overview of Nano- and Microencapsulation for Foods. *Nano- and Microencapsulation for Foods*, 1–14.

Jin, L., W., Park, J., H., & Robinson, J., R. (2000). Bioadhesive-Based Dosage Forms: The Next Generation. *Journal of Pharmaceutical Sciences*. 89 (7): 850–66.

Lakowicz, J.R. (2006) Principles of Fluorescence Spectroscopy. 3rd ed. Springer: New York

Li-Chan, E. C. (2015). Bioactive peptides and protein hydrolysates: research trends and challenges for application as nutraceuticals and functional food ingredients. *Current Opinion in Food Science*, 1, 28–37.

Liu, Z., Jiao, Y., Wang, Y., Zhou, C., & Zhang, Z. (2008). Polysaccharides-based nanoparticles as drug delivery systems. *Advanced Drug Delivery Reviews*, 60(15), 1650–1662.

Livney, Y. D. (2010). Milk proteins as vehicles for bioactives. *Current Opinion in Colloid & Interface Science*, 15(1-2), 73–83.

Li, Q., Lan, H., & Zhao, Z. (2018). Protection effect of sodium alginate against heat-induced structural changes of lactoferrin molecules at neutral pH. LWT. - *Food Science and Technology*

Lönnerdal, B., & Lyer, S. (1995). Lactoferrin: Molecular Structure and Biological Function. *Annual Review of Nutrition*, 15(1), 93–110.

Loveday, S. M., Wang, X. L., Rao, M. A., Anema, S. G., Creamer, L. K., & Singh, H. (2010). Tuning the properties of β-lactoglobulin nanofibrils with pH, NaCl and CaCl2. *International Dairy Journal*, 20(9), 571–579.

Loveday, S. M., Wang, X. L., Rao, M. A., Anema, S. G., & Singh, H. (2012). β-Lactoglobulin nanofibrils: Effect of temperature on fibril formation kinetics, fibril morphology and the rheological properties of fibril dispersions. *Food Hydrocolloids*, 27(1), 242–249.

Madureira, A. R., Tavares, T., Gomes, A. M. P., Pintado, M. E., & Malcata, F. X. (2010). Invited review: Physiological properties of bioactive peptides obtained from whey proteins. *Journal of Dairy Science*, 93(2), 437–455.

Magdeldin, S., Enany, S., Yoshida, Y., Xu, B., Zhang, Y., Zureena, Z., Lokamani, I., Yaoita, E., & Yamamoto, T. (2014). Basics and recent advances of two dimensional- polyacrylamide gel electrophoresis. *Clinical Proteomics*, 11(1), 16.

Maltais, A., Remondetto, G. E., & Subirade, M. (2009). Soy protein cold-set hydrogels as controlled delivery devices for nutraceutical compounds. *Food Hydrocolloids*, 23(7), 1647–1653.

Martins, J. T., Santos, S. F., Bourbon, A. I., Pinheiro, A. C., González-Fernández, Á., Pastrana, L. M., Cerqueira, M. A., & Vicente, A. A. (2016). Lactoferrin-based nanoparticles as a vehicle for iron in food applications – Development and release profile. *Food Research International*, 90, 16–24.

Mashaghi, S., Jadidi, T., Koenderink, G., & Mashaghi, A. (2013). Lipid Nanotechnology. *International Journal of Molecular Sciences*, 14(2), 4242–4282.

Matalanis, A., Jones, O. G., & McClements, D. J. (2011). Structured biopolymer-based delivery systems for encapsulation, protection, and release of lipophilic compounds. *Food Hydrocolloids*, 25(8), 1865–1880.

Mohan, P. R. K., Sreelakshmi, G., Muraleedharan, C. V., & Joseph, R. (2012). Water soluble complexes of curcumin with cyclodextrins: Characterization by FT-Raman spectroscopy. *Vibrational Spectroscopy*, 62, 77–84. 5

Morris, V. J. (2011). Emerging Roles of Engineered Nanomaterials in the Food Industry. *Trends in Biotechnology* 29 (10): 509–516.

Movasaghi, Z., Rehman, S., & ur Rehman, D. I. (2008). Fourier Transform Infrared (FTIR) Spectroscopy of Biological Tissues. *Applied Spectroscopy Reviews*, 43(2), 134–179.

Munin, A., & Edwards-Lévy, F. (2011). Encapsulation of Natural Polyphenolic Compounds; a Review. *Pharmaceutics*, 3(4), 793–829.

Nualkaekul, S., Cook, M. T., Khutoryanskiy, V. V., & Charalampopoulos, D. (2013). Influence of encapsulation and coating materials on the survival of Lactobacillus plantarum and Bifidobacterium longum in fruit juices. *Food Research International*, 53(1), 304–311.

Pando, D., Beltrán, M., Gerone, I., Matos, M., & Pazos, C. (2015). Resveratrol entrapped niosomes as yoghurt additive. *Food Chemistry*, 170, 281–287.

Patel, A. R., & Bhandari, B. (2014). Nano- and Microencapsulation of Vitamins. *Nano- and Microencapsulation for Foods*, 223–248. doi:10.1002/97811182.

Patra, D., & Barakat, C. (2011). Synchronous fluorescence spectroscopic study of solvatochromic curcumin dye. *Spectrochimica Acta Part A: Molecular and Biomolecular Spectroscopy*, 79(5), 1034–1041.

Pennington, S. R., Wilkins, M. R., Hochstrasser, D. F., & Dunn, M. J. (1997). Proteome analysis: from protein characterization to biological function. *Trends in Cell Biology*, 7(4), 168–173.

Pezeshki, A., Ghanbarzadeh, B., Mohammadi, M., Fathollahi, I., & Hamishehkar, H. (2014). Encapsulation of Vitamin A Palmitate in Nanostructured Lipid Carrier (NLC) -Effect of Surfactant Concentration on the Formulation Properties. *Advanced Pharmaceutical Bulletin* 4 (Suppl 2): 563–68.

Pinheiro, A. C., Bourbon, A. I., Cerqueira, M. A., Maricato, É., Nunes, C., Coimbra, M. A., & Vicente, A. A. (2015). Chitosan/fucoidan multilayer nanocapsules as a vehicle for controlled release of bioactive compounds. *Carbohydrate Polymers*, 115, 1–9.

Qiu, Y., & Park, K. (2012). Environment-sensitive hydrogels for drug delivery. *Advanced Drug Delivery Reviews*, 64, 49–60.

Quirós-Sauceda, A. E., Ayala-Zavala, J. F., Olivas, G. I., & González-Aguilar, G. A. (2014). Edible coatings as encapsulating matrices for bioactive compounds: a review. *Journal of Food Science and Technology*, 51(9), 1674–1685.

Ramos, O. L., Pereira, R. N., Martins, A., Rodrigues, R., Fuciños, C., Teixeira, J. A., Pastrana, L. M., Xavier Malcata, F., & Vicente, A. A. (2015). Design of whey protein nanostructures for incorporation and release of nutraceutical compounds in food. *Critical Reviews in Food Science and Nutrition*, 57(7), 1377–1393.

Ray (née Raman), P., Rielly, C. D., & Stapley, A. G. F. (2017). A freeze-drying microscopy study of the kinetics of sublimation in a model lactose system. *Chemical Engineering Science*, 172, 731–743.

Reimer L. (1993). Introduction. Springer Series in Optical Sciences, 1–18.

Rivera, M. C., Pinheiro, A. C., Bourbon, A. I., Cerqueira, M. A., & Vicente, A. A. (2015). Hollow chitosan/alginate nanocapsules for bioactive compound delivery. *International Journal of Biological Macromolecules*, 79, 95–102.

Rocha, G. A., Fávaro-Trindade, C. S., & Grosso, C. R. F. (2012). Microencapsulation of lycopene by spray drying: Characterization, stability and application of microcapsules. *Food and Bioproducts Processing*, 90(1), 37–42.

Rubinstein, M. and Colby, R. H. (2003). Polymer Physics (Vol.). Oxford University Press, Oxford.

Sabareesh, K. P. V. (2006). Dynamic Light Scattering Studies on Photo Polymerized and Chemically Cross-linked Polyacrylamide Hydrogels. *AIP Conference Proceedings.*

Sadeghi, R., Kalbasi, A., Emam-jomeh, Z., Razavi, S. H., Kokini, J., & Moosavi-Movahedi, A. A. (2013). Biocompatible nanotubes as potential carrier for curcumin as a model bioactive compound. *Journal of Nanoparticle Research,* 15(11).

Schmitz, K. S., & Phillies, G. D. J. (1991). An Introduction to Dynamic Light Scattering by Macromolecules. *Physics Today*, 44(5), 66–66.

Shen, L., & Patel, M. K. (2008). Life Cycle Assessment of Polysaccharide Materials: A Review. *Journal of Polymers and the Environment*, 16(2), 154–167.

Shome, S., Talukdar, A. D., Choudhury, M. D., Bhattacharya, M. K., & Upadhyaya, H. (2016). Curcumin as potential therapeutic natural product: a nanobiotechnological perspective. *Journal of Pharmacy and Pharmacology,* 68(12), 1481–1500.

Siebert, K. J., Troukhanova, N. V., & Lynn, P. Y. (1996). Nature of Polyphenol–Protein Interactions. *Journal of Agricultural and Food Chemistry,* 44(1), 80–85.

Sneharani, A. H., Karakkat, J. V., Singh, S. A., & Rao, A. G. A. (2010). Interaction of Curcumin with β-Lactoglobulin—Stability, Spectroscopic Analysis, and Molecular Modeling of the Complex. *Journal of Agricultural and Food Chemistry*, 58(20), 11130–11139.

Sozer, N., & Kokini, J. L. (2009). Nanotechnology and its applications in the food sector. *Trends in Biotechnology*, 27(2), 82–89.

Stănciuc, N., Aprodu, I., Râpeanu, G., van der Plancken, I., Bahrim, G., & Hendrickx, M. (2013). Analysis of the Thermally Induced Structural Changes of Bovine Lactoferrin. *Journal of Agricultural and Food Chemistry*, 61(9), 2234–2243.

Stănciuc, N., Aprodu, I., Râpeanu, G., & Bahrim, G. (2012). Fluorescence spectroscopy and molecular modeling investigations on the thermally induced structural changes of bovine β-lactoglobulin. *Innovative Food Science & Emerging Technologies*, 15, 50–56.

Tajkarimi, M. M., Ibrahim, S. A., & Cliver, D. O. (2010). Antimicrobial herb and spice compounds in food. *Food Control,* 21(9), 1199–1218.

Talari, A. C. S., Martinez, M. A. G., Movasaghi, Z., Rehman, S., & Rehman, I. U. (2016). Advances in Fourier transform infrared (FTIR) spectroscopy of biological tissues. *Applied Spectroscopy Reviews,* 52(5), 456–506.

Tavares, G. M., Croguennec, T., Carvalho, A. F., & Bouhallab, S. (2014). Milk proteins as encapsulation devices and delivery vehicles: Applications and trends. *Trends in Food Science & Technology*, 37(1), 5–20.

Chen, G., Wang, H., Zhang, X., & Yang, S.-T. (2014). Nutraceuticals and Functional Foods in the Management of Hyperlipidemia. *Critical Reviews in Food Science and Nutrition*, 54(9), 1180–1201.

Teng, Z., Luo, Y., & Wang, Q. (2012). Nanoparticles Synthesized from Soy Protein: Preparation, Characterization, and Application for Nutraceutical Encapsulation. *Journal of Agricultural and Food Chemistry*, 60(10), 2712–2720.

Teng, Z., Li, Y., & Wang, Q. (2014). Insight into Curcumin-Loaded β-Lactoglobulin Nanoparticles: Incorporation, Particle Disintegration, and Releasing Profiles. *Journal of Agricultural and Food Chemistry*, 62(35), 8837–8847.

Totosaus, A., Montejano, J. G., Salazar, J. A., & Guerrero, I. (2002). A review of physical and chemical protein-gel induction. *International Journal of Food Science and Technology*, 37(6), 589–601.

Veerman, C., Sagis, L. M. C., Heck, J., & van der Linden, E. (2003). Mesostructure of fibrillar bovine serum albumin gels. *International Journal of Biological Macromolecules*, 31(4-5), 139–146.

Weckhuysen, B., M. (2004). CHAPTER 12 Ultraviolet-Visible Spectroscopy. 255–70.

Weiss, S. (1999). Fluorescence Spectroscopy of Single Biomolecules. *Science*, 283(5408), 1676–1683.

Wilde, S. C., Keppler, J. K., Palani, K., & Schwarz, K. (2016). β -Lactoglobulin as nanotransporter for allicin: Sensory properties and applicability in food. *Food Chemistry,* 199, 667–674.

Zou, L., Zheng, B., Zhang, R., Zhang, Z., Liu, W., Liu, C., Xiao, H., & McClements, D. J. (2016). Food-grade nanoparticles for encapsulation, protection and delivery of curcumin: comparison of lipid, protein, and phospholipid nanoparticles under simulated gastrointestinal conditions. *RSC Advances,* 6(4), 3126–3136.